Journal of Asian Earth Sciences 137 (2017) 163–179

Contents lists available at ScienceDirect

Journal of Asian Earth Sciences

journal homepage: www.elsevier.com/locate/jseaes

U–Pb, Re–Os and Ar–Ar dating of the Linghou polymetallic deposit, Southeastern China: Implications for metallogenesis of the Qingzhou–Hangzhou metallogenic belt

Yanwen Tang [a,*], Yuling Xie [b], Liang Liu [a], Tingguan Lan [a], Jianling Yang [c], Meffre Sebastien [d], Rongchao Yin [c], Songsong Liang [c], Limin Zhou [e]

[a] State Key Laboratory of Ore Deposit Geochemistry, Institute of Geochemistry, Chinese Academy of Sciences, Guiyang 550081, China
[b] School of Civil and Environmental Engineering, University of Science and Technology Beijing, Beijing 100083, China
[c] Hangzhou Jiantong Group Co., Ltd, Jiande 311608, China
[d] CODES ARC Centre of Excellence in Ore Deposits, University of Tasmania, Hobart, TAS 7001, Australia
[e] National Center of Rock and Mineral Analysis, CAGS, Beijing 100037, China

ARTICLE INFO

Article history:
Received 11 May 2016
Received in revised form 5 February 2017
Accepted 7 February 2017
Available online 9 February 2017

Keywords:
Qinzhou–Hangzhou metallogenic belt (QHMB)
Zircon U–Pb dating
Molybdenite Re–Os dating
Hydrothermal muscovite Ar–Ar dating
Ore genesis

ABSTRACT

The Qingzhou–Hangzhou metallogenic belt (QHMB) in Southeastern China has gained increasingly attention in recent years. However, due to the lack of reliable ages on intrusions and associated deposits in this belt, the tectonic setting and metallogenesis of the QHMB have not been well understood. The Linghou polymetallic deposit in northwestern Zhejiang Province is one of the typical deposits of the QHMB. According to the field relationships, this deposit consists of the early Cu–Au–Ag and the late Pb–Zn–Cu mineralization stages. Molybdenite samples with a mineral assemblage of molybdenite–chalcopyrite–pyrite ± quartz are collected from the copper mining tunnel near the Cu–Au–Ag ore bodies. Six molybdenite samples give the Re–Os model ages varying from 160.3 to 164.1 Ma and yield a mean age of 162.2 ± 1.4 Ma for the Cu–Au–Ag mineralization. Hydrothermal muscovite gives a well-defined Ar–Ar isochron age of 160.2 ± 1.1 Ma for the Pb–Zn–Cu mineralization. Three phases of granodioritic porphyry have been distinguished in this deposit, and LA–ICP–MS zircon U–Pb dating shows that they have formed at 158.8 ± 2.4 Ma, 158.3 ± 1.9 Ma and 160.6 ± 2.1 Ma, comparable to the obtained ages of the Cu–Au–Ag and Pb–Zn–Cu mineralization. Therefore, these intrusive rocks have a close temporal and spatial relationship with the Cu–Au–Ag and Pb–Zn–Cu ore bodies. The presences of skarn minerals (e.g., garnet) and vein-type ores, together with the previous fluid inclusion and H–O–C–S–Pb isotopic data, clearly indicate that the Cu–Au–Ag and Pb–Zn–Cu mineralization are genetically related to these granodiorite porphyries. This conclusion excludes the possibility that this deposit is of "SEDEX" type and formed in a sag basin of continental rifts setting as previously proposed. Instead, it is proposed that the Linghou polymetallic and other similar deposits in the QHMB, such as the 150–160 Ma Yongping porphyry-skarn Cu–Mo, Dongxiang porphyry? Cu, Shuikoushan/Kangjiawang skarn Pb–Zn, Fozichong skarn Pb–Zn and Dabaoshan porphyry-skarn deposits are of magmatic-hydrothermal origin and likely formed in a subduction-related setting. This work provides new insight that these intrusion-related deposits (e.g., porphyry and skarn types) of middle to late Jurassic age can be the most important targets for exploration in the QHMB.

1. Introduction

The Qinzhou–Hangzhou metallogenic belt (QHMB), which was once considered to spatially overlap with the suture zone between the Yangtze and Cathaysian Blocks (Fig. 1), is considered to be one of the most important polymetallic belts in China. A dozen of large or super-large ore deposits have occurred in this belt, such as the famous Dexing porphyry Cu–Mo–Au, Jinshan Au and Yinshan Pb–Zn–Cu polymetallic deposits (Mao et al., 2011a,b; Li et al., 2011, 2012; Zhou et al., 2013; Guo et al., 2012; Wang et al., 2011, 2013a, 2015a, 2012b), Xianglushan skarn W (Zhang et al., 2008; Chen and Zhou, 2012), Dahutang porphyry W (Feng et al., 2012; Mao et al., 2013), Yongping porphyry-skarn Cu–Mo (Li et al.,

* Corresponding author.
E-mail address: tyw_xt@126.com (Y. Tang).

http://dx.doi.org/10.1016/j.jseaes.2017.02.016
1367-9120/

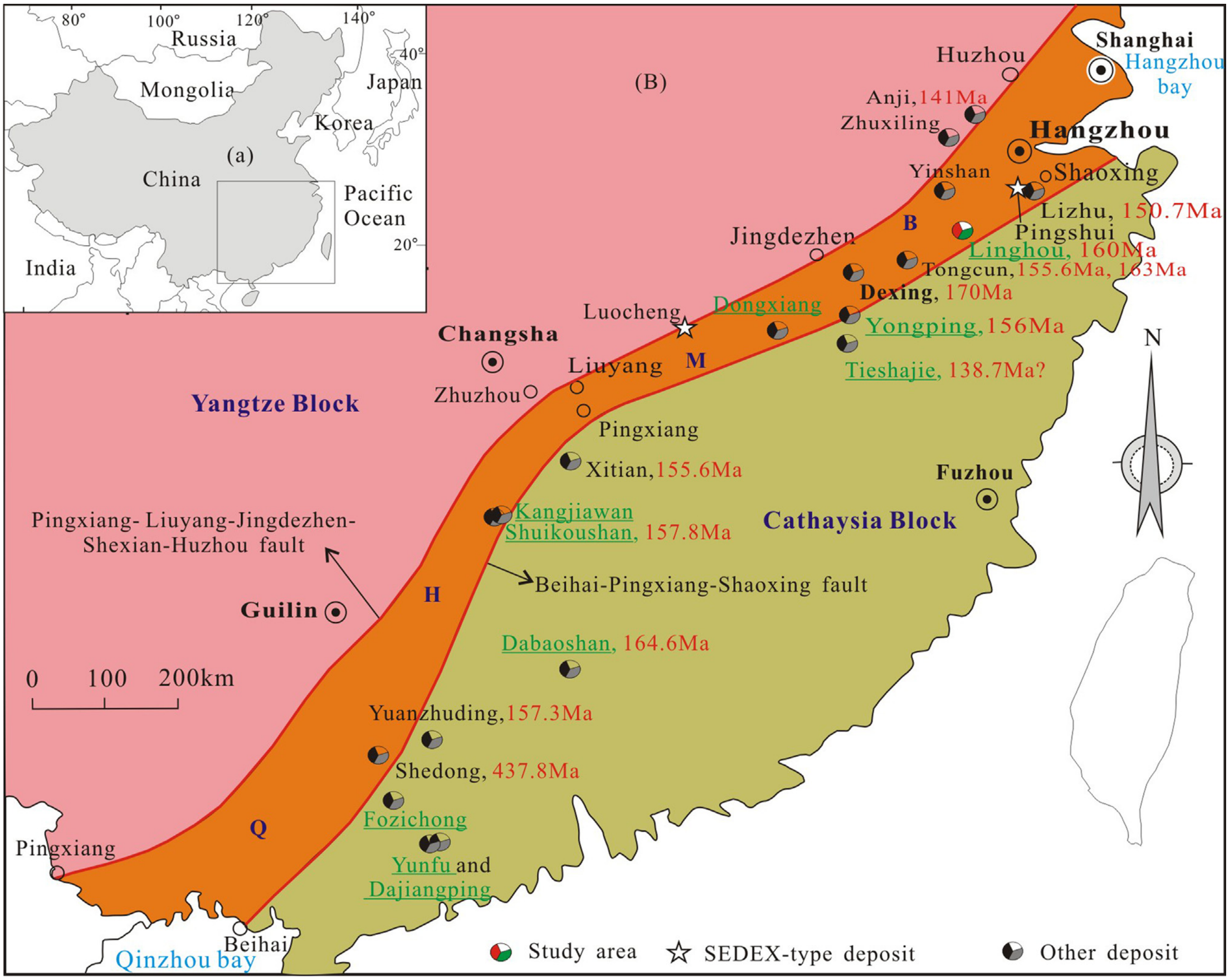

Fig. 1. Distribution of the skarn and porphyry type deposits in the Qinzhou–Hangzhou metallogenic belt (QHMB) (modified from Yang and Mei, 1997 and Mao et al., 2011a).

2013a), and Zhangshiba Pb–Zn deposits (Lu et al., 2005). As a typical metallogenic belt in Southeastern China, the QHMB has been studied for many years (Zhou et al., 2012; Mao et al., 2011a,b, 2013; Xu et al., 2012, 2015). However, this belt has not been fully recognized until recently, and its metallogenesis and geological setting are still poorly understood (Mao et al., 2011a; Xu et al., 2012, 2015; He et al., 2015). In particular, the extension and the formation and evolution history of this belt has been debating for three decades (Li, 2000; He et al., 2005, 2015; Shu, 2006; Yang et al., 2009; Mao et al., 2011a; Xu et al., 2012, 2015). Previous studies in the QHMB mostly focused on the typical deposits in the middle section (about from Guilin city to the Dexing area in Fig. 1), and the spatial-temporal distribution of magmatic and mineralization events have been summarized and reported (Mao et al., 2011a, 2013). However, most of magmatic and related mineralization events in the northeast QHMB (from the Dexing area to Hangzhou city in Fig. 1) have been poorly summarized. Moreover, a dozen of typical deposits (marked with green[1] color and underline in Fig. 1) in the belt were previously considered to be SEDEX-type on the basis of the so-called "stratiform" orebodies and "laminate textures" of the ores (Y.Z. Zhou et al., 2015; Xu et al., 2015). However, due to the lack of precise mineralization age, it is not clear if these deposits are syngenetic or intrusion-related, particularly when some of the ores are tightly metamorphosed or deformed.

The Linghou copper–lead–zinc polymetallic deposit (previously named Jiande copper deposit) in the northeast QHMB is an important medium-sized deposit and is located ca. 120 km southwest of Hangzhou city in Zhejiang Province, Southeastern China (Fig. 1). The early discovered Cu–Au–Ag orebodies in the Linghou ore field were almost exhausted after forty years of mining. Fortunately, new Cu–Au–Ag and Pb–Zn–Cu orebodies have been found in the Songkengwu ore field since 2003 (Yu, 2010). Previous studies focused on the Cu–Au–Ag orebodies are available (Xu et al., 1981; Cao et al., 1988; Zhou and Yu, 1983; Liu et al., 1996). However, due to the lack of reliable ages, the genetic relationship between magmatism and mineralization in the Linghou polymetallic deposit is still controversial (Xu et al., 1981; Cao et al., 1988; Zhou and Yu, 1983; Liu et al., 1996). Recently, based on the new geological evidences, fluid inclusion, and H–O–C–S–Pb isotopic data, the Linghou polymetallic deposit was interpreted to be intrusion-related, and furthermore, two mineralization events of the early Cu–Au–Ag orebodies and the late Pb–Zn–Cu ore bodies or veins were obviously identified (Tang et al., 2015a; H. Chen et al., 2016).

The aim of this paper is to present new age for three granodiorite porphyry phases, the molybdenite Re–Os age for the Cu–Au–Ag mineralization and the hydrothermal muscovite Ar–Ar age for

[1] For interpretation of color in Figs. 1 and 5, the reader is referred to the web version of this article.

Pb–Zn–Cu mineralization to discuss the genetic relationship between magmatism and mineralization events in the Linghou deposit. Moreover, the recent results on the typical deposits in the QHMB were summarized to better understand the magmatic-hydrothermal system of this belt and provide the new implications for tectonic setting and regional exploration in the QHMB.

2. Geological background

The QHMB, which extends from the Qinzhou Bay of Guangxi Province to the Hangzhou Bay of Zhejiang Province, is about 2000 km long and 100–150 km wide (Yang and Mei, 1997). This belt is bounded by the Pingxiang–Liuyang–Jingdezhen–Shexian–Huzhou fault in the north and the Beihai–Pingxiang–Shaoxing fault in the south (Fig. 1). The middle and southwest QHMB (from Guilin to Beihai city in Fig. 1) has been considered to widen to include Xitian, Yunfu (Dajianping) and Dabaoshan deposits (Zhou et al., 2012). The QHMB was interpreted to have resulted from the collision and extension between the Yangtze and Cathaysian Blocks. However, these two blocks were connected firstly during the Neoproterozoic period (about 825 Ma) (Hong et al., 2002; Shu, 2006; Yang et al., 2009). This period is characterized by formation of volcanic arc igneous rocks (e.g., spilite– and quartz– keratophyre) in the basement rocks, such as the Shuanxiwu group in the northeast QHMB, accompanied with coeval SEDEX Cu, Pb–Zn deposits, such as Pingshui and Luocheng copper deposits (Xu et al., 2015; Y.Z. Zhou et al., 2015). There was no evidence to show that the QHMB had reactivated during the Silurian and Triassic period (Mao et al., 2011a). Correspondingly, the clastic and carbonate rocks of neritic facies have been formed during Devonian–middle Triassic Period, and the coal and few strata–bound polymetallic deposits of deep–water phases occurred along the ancient faults in Permian period (Yang and Mei, 1997; Li, 2000). Subsequently, due to the conversion of tectonic regime from the Tethys to Paleo–Pacific, this belt had been reactivated several times during Yanshanian deformations (about from 135 to 205 Ma) (Yang and Mei, 1997; Li, 2000; He et al., 2005, 2015; Mao et al., 2011a). However, the accurate time when the Paleo–Pacific plates subducted beneath the Eurasian continent is under debate. Dong et al. (2008) believed that the time should be 165 Ma, whereas Mao et al. (2013) constrained it to 175 Ma. Recently, Sun et al. (2015) confirmed that the initial Paleo–Pacific subduction occurred in 275 Ma. In summary, the QHMB was controlled by the inland compression associated with the subduction and collision from the Paleo–Pacific plate (Yang et al., 2009; Mao et al., 2009; Li et al., 2013b). In particular, the middle and northeast QHMB also experienced the local extension events which were indicated by adakitic porphyries in the Dexing deposit (Wang et al., 2006) and A–type granitoids in the Lizhu and Nanling areas (Hua et al., 2005; Jia et al., 2014). Till now, most of the Mesozoic tectono-magmatism events in the QHMB were considered to be related to the interaction between the Eurasian and Paleo-Pacific plates (Shu and Zhou, 2002; Wu et al., 2003; Zhou et al., 2006; Yang et al., 2009; Mao et al., 2009; Zheng et al., 2013; He et al., 2015). Several models have been proposed, including: (1) the tear-off and remelting of the subducted Izanagi Plate (170–160 Ma), and upwelling of asthenospheric magma and extensive mantle–crust interaction possibly induced by the plate window (160–150 Ma) (Mao et al., 2011a, 2013); (2) lithosphere extension and thinning, and underplating of mantle–derived magmas (Hua et al., 2005; Yang et al., 2009); (3) lithosphere extension and partial melting of delaminated lower crust (Wang et al., 2004). These models above were believed to give rise to those intensive intracontinental tectonic-magmatic activities and metallogenesis in Southeastern China (Wang et al., 2004; Hua et al., 2005; Seton and Müller, 2008; Mao et al., 2009, 2013; Xiao et al., 2010; Zhang et al., 2013; He et al., 2015). Generally, the NNE and NE trending faults in the QHMB controlled the magmatic activities and the mineralization events in Yanshanian (Yang and Mei, 1997; Yang et al., 2009). Most of the typical deposits, such as the Dexing porphyry Cu and Yongpin porphyry-skarn Cu deposits, have formed in this period.

3. Geology of the Linghou polymetallic deposit

The strata in the Linghou area are divided into the Upper Devonian Xihu and Zhuzangwu Formations and the Upper Carboniferous Huanglong Formation (BGMRZP, 1989), with the general strike of NE–SW. The Xihu Formation, 120–130 m thick, is only exposed in two limbs of the Songkengwu syncline (Fig. 2) and mainly consists of the quartz sandstone. The Zhuzangwu Formation is exposed in the two limbs of the Songkengwu syncline as well as the axis of the Tongshan anticline (Fig. 2), which is estimated to be 64–142 m thick and mainly consists of sandstone bearing shale and fine sandstone. The Upper and Lower Huanglong Formation is mainly exposed in the axis part of the Songkengwu syncline and consists of the pure limestone ($\sim$185 m thick) and limy dolomite (30–35 m thick), respectively. Notably, parts of the sedimentary successions have been altered and metamorphosed. The carbonate rocks, including marble and dolomite, were the main host rocks for the Cu–Au–Ag and Pb–Zn–Cu mineralization (Fig. 2).

The structures in this study region are mainly products of the Indosinian and Yanshanian orogenies. The early Indosinian orogeny gave rise to the Songkengwu syncline, Tongshan anticline, and some coeval faults, whereas the late Yanshanian orogeny commonly reactivated the early structures. Therefore, in the Songkengwu ore field, the principal structures include the Songkengwu syncline and several NE–SW, NW–SE and EW trending faults. Some of them were occupied by Yanshannian granitic intrusions and orebodies (Fig. 2).

Ore bodies in the Linghou deposit have close spatial relationships with the intrusive rocks (Figs. 2 and 4). Previous studies considered that there were multi-stage intrusions in the Linghou area (Xu et al., 1981; Zhou and Yu, 1983; Yu, 2010). For example, the early biotite granodiorite porphyry, granodiorite porphyries (phase 1 and phase 2) and other two stages of andesite were reported in Chinese by Xu et al. (1981). Although primary structures and textures of these igneous rocks are difficult to be identified due to the strong alteration, there is a consensus that the granodiorites are the principal intrusive rocks to control the mineralization in the Linghou mine (Xu et al., 1981; Zhou and Yu, 1983; Yu, 2010; L. Chen et al., 2013; Jia et al., 2014). In the Songkengwu ore field, the intrusive rocks occupy an axis and two limbs of the syncline and strike NE–SW (Fig. 2).

The wallrock alterations in roughly chronological order are skarnization, phyllic alteration, silicification and carbonatization in the Linghou mining area. In skarnization, the garnet is often replaced by chlorite, epidote and calcite (Fig. 3). The phyllic alteration is well developed in granitic rocks and characterized by disseminated sericite and quartz, with minor pyrite and chalcopyrite. Silicification is closely related to the Cu–Au–Ag mineralization and characterized by the quartz in ores or quartz + pyrite + chalcopyrite veins in strata and granitic rocks. The carbonatization is very common in the whole mining area, which is often characterized by early recrystallization of dolomite + calcite associated with the Pb–Zn–Cu mineralization, the calcite cluster in hydrothermal calcite cave near the Pb–Zn–Cu orebodies and the late calcite (±galena) veins or veinlets across the ore and granitic rocks.

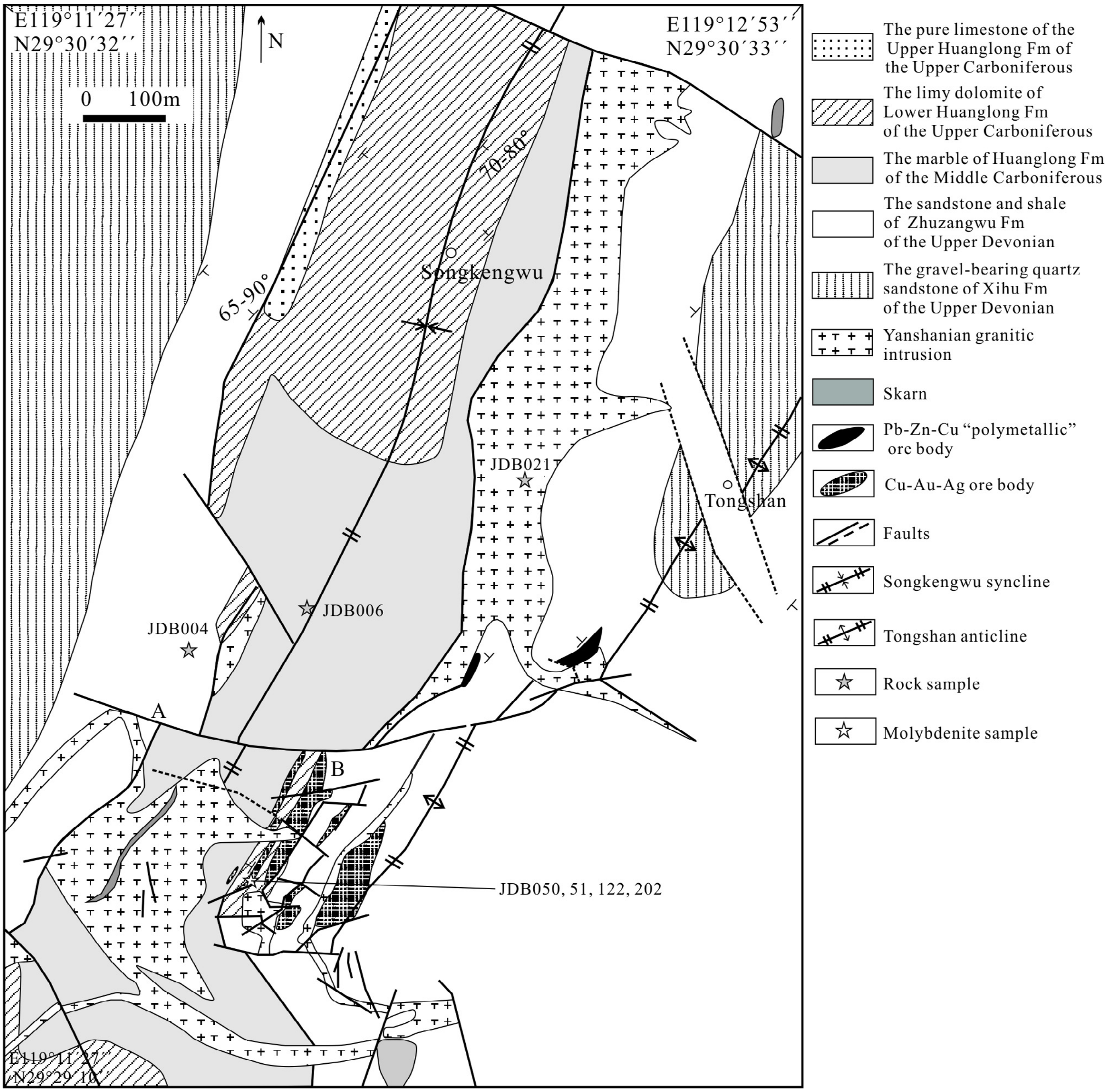

Fig. 2. Geological sketch map of the Linghou Cu–Pb–Zn polymetallic deposit (modified from Chen, 2005).

The Linghou deposit contains the early Cu–Au–Ag mineralization and late Pb–Zn–Cu mineralization which is commonly superimposed on the early Cu–Au–Ag mineralization, forming the Pb–Zn–Cu "polymetallic" orebodies (Figs. 2 and 4a). Distributions of both stages of mineralization are commonly controlled by the structures and lithologies, and thus these mineralization are characterized by ore veins or irregular ore lenses with sharp boundaries against the wall rocks.

The Cu–Au–Ag orebodies are situated in the southeastern limb of the Songkengwu anticline (Fig. 2). The primary ores are mainly massive and banded, and contain ore minerals dominated by chalcopyrite, bornite and pyrite, with minor gold, silver minerals (only be found in chalcopyrite), sphalerite and molybdenite. Gangue minerals are quartz, minor garnet, epidote, chlorite, calcite and dolomite. The sulfide minerals are mainly present as massive, banded and vein within the host rock, with rare veinlet-disseminated structures.

The Pb–Zn–Cu "polymetallic" orebodies occur in the center of the Songkengwu anticline (Fig. 2). The massive and banded ores consist of sphalerite, chalcopyrite, pyrite and galena, with calcite and dolomite as gangue minerals. Those sulfide minerals are mainly present as massive, banded and vein bodies within the host rocks.

4. Sample descriptions

The samples for zircon U–Pb dating were collected from three granodiorite porphyry phases in the Songkengwu ore field in the underground tunnel (Fig. 5). Their locations have been indicated in Fig. 2.

Biotite granodiorite porphyry: This granodiorite porphyry has a gray-green color due to the intensive chlorite alteration. JDB021 was collected from this phase for zircon U–Pb dating. This rock

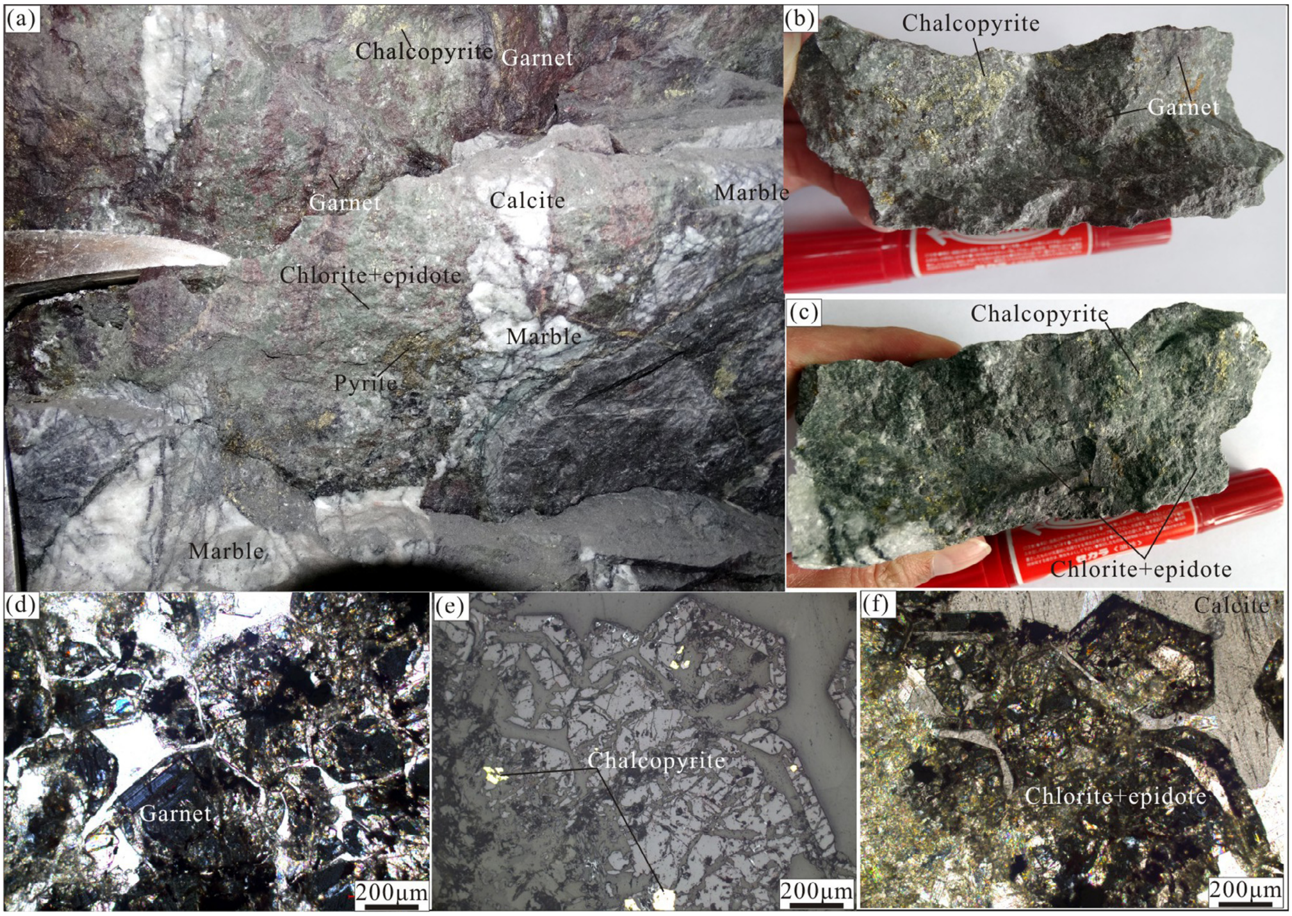

Fig. 3. Garnet and chalcopyrite in skarn at the connect zone between the carbonate Formation and the Cu–Au–Ag ore bodies. (a) Calc-silicate (skarn) alteration occurred at the connect zone between the carbonate Formation and the Cu–Au–Ag ore bodies; (b) and (c) The photographs for the hand specimens of skarn; (d) The residual garnet in cross-polarized light; (e) Chalcopyrite in garnet in reflected light; (f) Garnet was replaced by chlorite + epidote + calcite.

shows massive structure and porphyritic texture (Fig. 5a–c), and are dominantly composed of the phenocrysts with plagioclase (~40 vol.%), potash feldspar (~10 vol.%), biotite and hornblende (~15 vol.%), quartz (~5 vol.%) and the matrixes of 30% in volume. The phenocrysts (~80 vol.%) have the grain size ranging from 0.1 to 1.0 mm, whereas the matrix (~20 vol.%) has the general grain size of ~0.02 mm.

Granodiorite porphyries (phase 1 and phase 2): These granodiorite porphyries are in gray-white color. Two samples of JDB004 (phase 1) and JDB006 (phase 2) were collected for zircon U–Pb dating. These rocks are characterized by massive structure, fine-grained porphyritic-like (Fig. 5d–f) or porphyritic (Fig. 5g–i) texture, with phenocrysts of feldspar (~35 vol.%), quartz (~5 vol.%) and biotite (~3 vol.%) and the matrixes of ~60% in volume. Most of the phenocrysts show the grain size varying from 0.1 to 1.0 mm, whereas the matrix has the grain size of less than 0.05 mm. Generally, the size of the matrix in JDB006 is smaller than JDB004.

Muscovite samples from the altered granodiorite porphyry (phase 2) were selected for Ar–Ar dating. They occur as euhedral aggregates with a diameter of ~10 mm and are intergrowth with hydrothermal pyrite and Pb–Zn vein (Fig. 6).

Six molybdenite samples for Re–Os dating were selected from the Cu–Au–Ag ore bodies (Fig. 2). One sample (JD122) was collected from a 2-cm-thick quartz–molybdenite–pyrite vein in the fractures, whereas other molybdenite samples were collected from quartz–molybdenite–pyrite–chalcopyrite or molybdenite (–pyrite) veinlet in marble, fine sandstone and shale (Fig. 7).

5. Analytical methods

5.1. LA–ICP–MS zircon U–Pb dating

In order to identify zircon internal textures and select target spots for U–Pb dating, the SEM cathodoluminescence (CL) images of zircons from these three samples were photographed by using a JSM–6510 electron microprobe coupled with a Gatan CL Detector at Beijing Geoanalysis Co., Ltd.

In-situ zircon U–Pb dating were performed on an Agilent 7500cs quadrupole ICPMS with a 193 nm Coherent Ar–F gas laser and the Resonetics S155 ablation cell at the University of Tasmania in Hobart. The downhole fractionation, instrument drift and mass bias correction factors for Pb/U ratios on zircons were calculated using 2 analyses on the primary (91500 standard of Wiedenbeck et al., 1995) and 1 analysis on each of the secondary standard zircons (Temora or GJ–1, Black et al., 2004 and Jackson et al., 2004) analysed at the beginning of the session and every 15 unknown zircons (roughly every half an hour) using the same spot size and conditions as used on the samples. The correction factor for the $^{207}Pb/^{206}Pb$ ratio was calculated using large spots of NIST610 analysed every 30 unknowns and corrected using the values recommended by Baker et al. (2004). Each analysis on the zircons began with a 30 s blank gas measurement followed by a further 30 s of analysis time when the laser was switched on. Zircons were sampled on 32 μm spots using the laser at 5 Hz and a density of approximately 2 J/cm^2. A flow of He carrier gas at a rate of

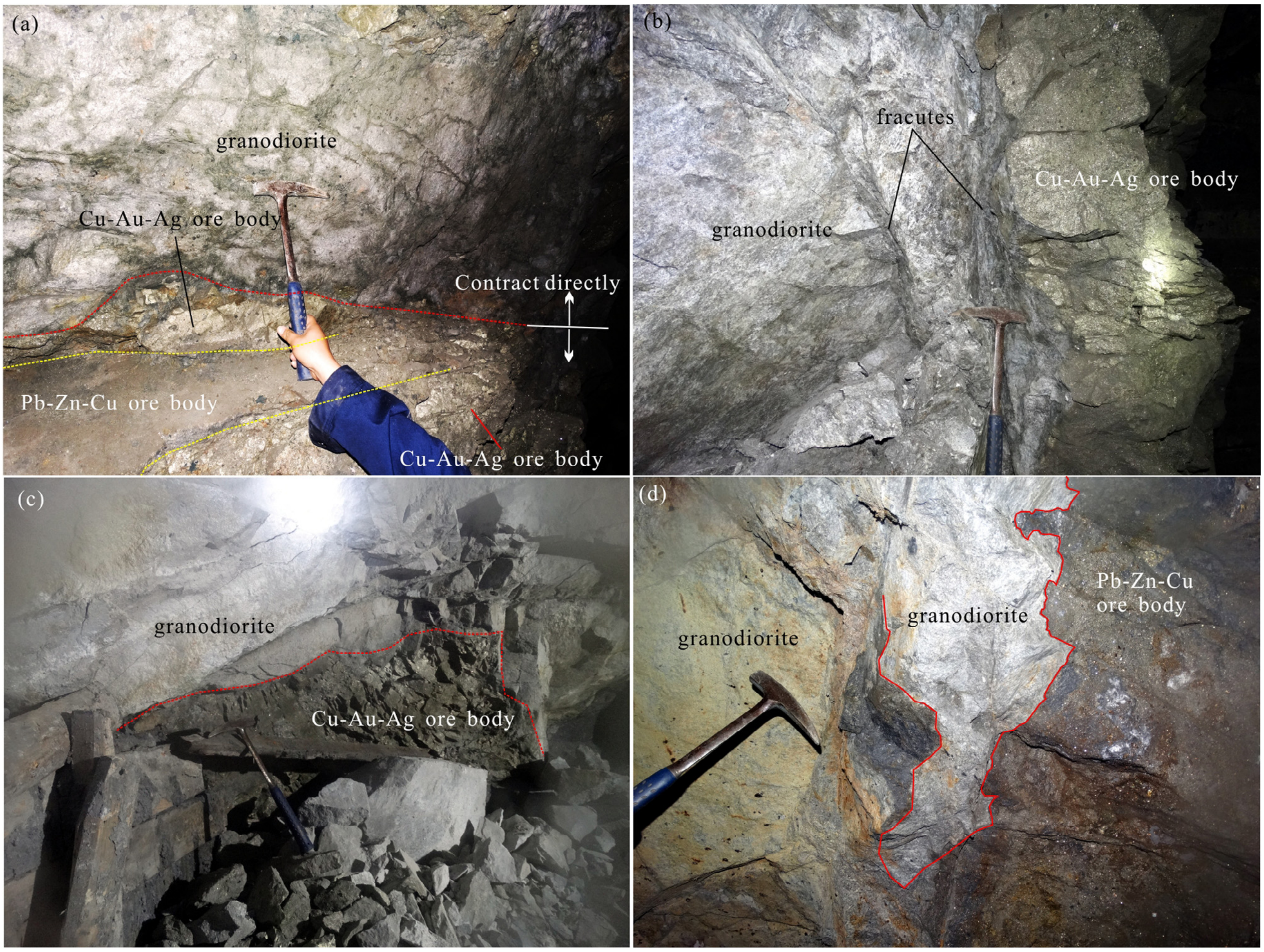

Fig. 4. The spatial relationship among the granodiorite porphyry, Cu–Au–Ag and Pb–Zn–Cu ore bodies. (a) The Pb–Zn–Cu ore body crosscut the Cu–Au–Ag ore body and both of them contact directly with the granodiorite porphyry in the shape of veins; (b) the contact zones are composed mainly of detrital rocks from the intrusion in the form of strike- slip surface; (c) the Cu–Au–Ag ore body contact directly with the granodiorite porphyry; (d) the Pb–Zn–Cu ore body crosscuts and entraps the granodiorite porphyry in the shape of "V".

0.35 L/min carried particles ablated by the laser out of the chamber to be mixed with Ar gas and carried to the plasma torch. Isotopes measured were ^{49}Ti, ^{56}Fe, ^{90}Zr, ^{178}Hf, ^{202}Hg, ^{204}Pb, ^{206}Pb, ^{207}Pb, ^{208}Pb, ^{232}Th and ^{238}U with each element being measured every 0.16 s with longer counting time on the Pb isotopes compared to the other elements. The data reduction used was based on the method outlined in detail in Black et al. (2004), Meffre et al. (2008), Paton et al. (2010) and Sack et al. (2011).

5.2. Molybdenite Re–Os dating

Molybdenite grains were handpicked individually under a binocular microscope to get over 95% pure molybdenite separates. Re–Os isotope analysis was performed on a TJA X-series ICP–MS at the Re–Os Laboratory in National Research Center of Geoanalysis, Chinese Academy of Geological Sciences in Beijing. The detailed analytical procedures have been described by Du et al. (1994, 2004). A model age of 221.4 ± 5.6 Ma, which is identical to the certified value of 220.6 ± 3.2 Ma, for the molybdenite standard GBW04435 has been obtained in this analysis. Blanks during these analyses are 0.0013 ± 0.0002 ppb for Re, 0.00089 ± 0.00012 ppb for Os and 0.00021 ± 0.00006 ppb for ^{187}Os. The ^{187}Re decay constant of 1.666×10^{-11} year^{-1} (Smoliar et al., 1996) is used to calculate the molybdenite model ages. Uncertainty in Re–Os model ages includes 1.02% uncertainty in the ^{187}Re decay constant and uncertainty in Re and Os concentrations which comprises weighing errors for both spike and sample, uncertainty in spike calibration and mass spectrometry analytical error.

5.3. Muscovite Ar–Ar dating

Muscovite separates were carefully handpicked under a binocular microscope, with purity over 99%. The sample separates, together with the monitoring standard samples were irradiated within a quartz vial in a nuclear reactor at the Chinese Institute of Atomic Energy, Beijing. Step-heating ^{40}Ar/^{39}Ar analyses were performed on noble gas mass spectrometry Helix SFT at the Analytical Laboratory, Beijing Research Institute of Uranium Geology, China. Procedural blanks are $<1 \times 10^{-15}$ mol at room temperature and $<1 \times 10^{-14}$ mol for ^{40}Ar. The monitor used in this work is the internal Fangshan biotite (ZBH–25) standard with an age of 132.7 ± 1.2 Ma and amphibole (GBW04418) standard with an age of 2060 ± 8 Ma, which were also irradiated. The decay constant for ^{40}K used in the calculation is 5.543×10^{-10} year^{-1} (Steiger and Jäger, 1977).

6. Results

6.1. Zircon U–Pb ages

Zircon U–Pb isotopic data for three granodiorite porphyry phases from the Songkengwu ore field are presented in Table 1. The zircon grains are commonly transparent, colorless, euhedral

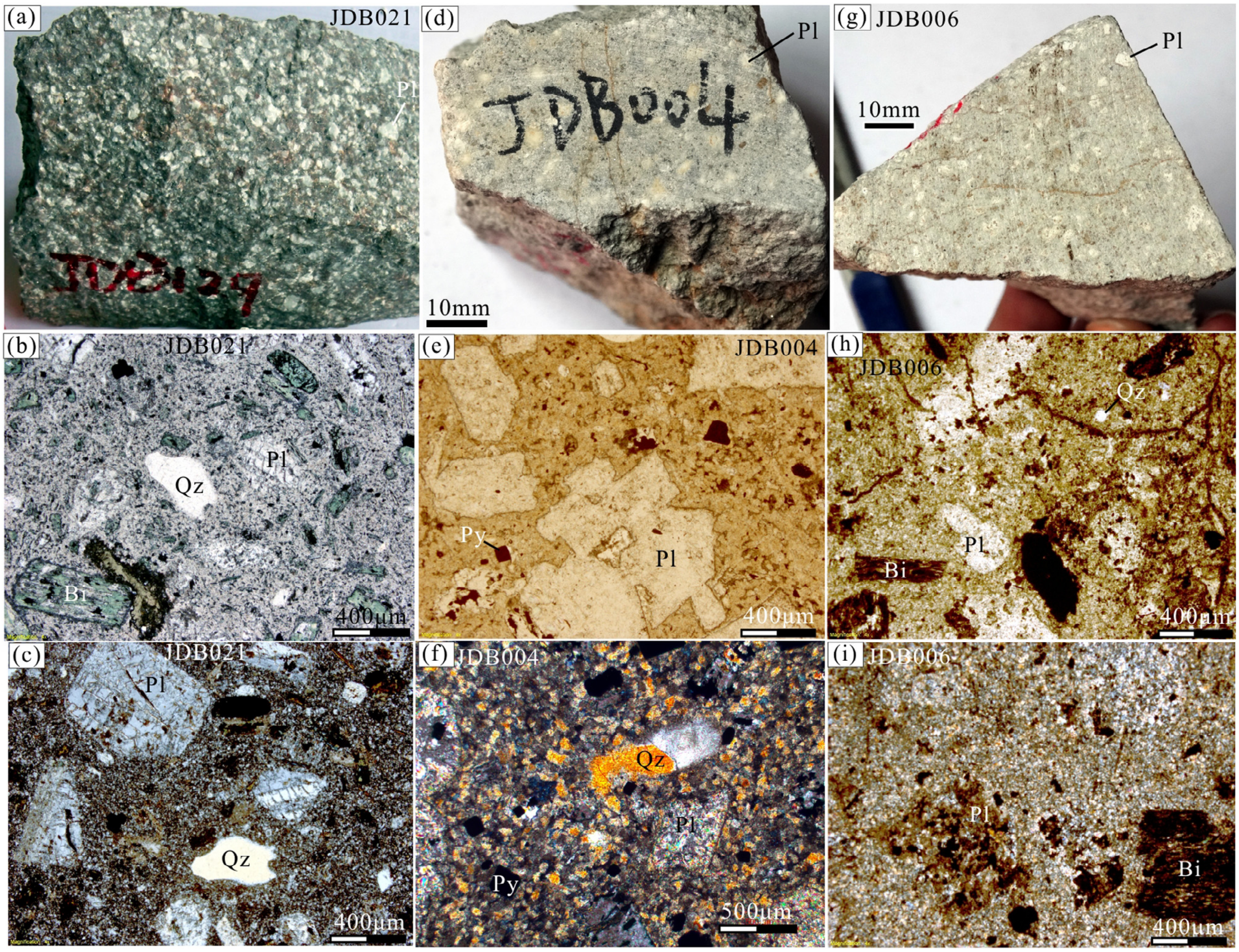

Fig. 5. Photographs and microphotos of three granodiorite porphyry phases in the Songkengwu ore field. (a–c) Biotite granodiorite porphyry, characterized by the chloritization of biotite and hornblende, subhedral plagioclase with double crystal and rounded-irregular quartz in the polarized light (b) and cross-polarized light (c); (d, e and f) Granodiorite porphyry (phase 1), characterized by little biotite, sericitization of subhedral and euhedral plagioclase, and rounded-irregular quartz in the polarized light (e) and cross-polarized light (f); (g, h and i) Granodiorite porphyry (phase 2), characterized by euhedral biotite, subhedral and euhedral plagioclase with sericitization, and rounded-irregular quartz in the polarized light (h) and cross-polarized light (i); Qz–quartz, Pl–plagioclase, Bi–biotite, Py–pyrite.

prismatic, with the lengths of 80–150 μm and the width/length ratios of 1:1–1:3. Most zircon grains show typical magmatic oscillatory zonings in CL images (Fig. 8). Zircons from samples of JDB021, JDB004 and JDB006 have consistent U and Th contents with Th/U ratios of 0.27–0.70, 0.32–0.71 (beside one value of 0.02) and 0.26–0.79, respectively (Table 1). These characteristics show that all zircon grains are magmatic origin.

Zircon U–Pb concordia diagrams for three granodiorite porphyry phases are shown in Fig. 9. Eleven analyses for the zircons grains from JDB021 yield $^{206}Pb/^{238}U$ ages ranging from 153.4 ± 2.1 to 164.2 ± 2.7 Ma, with a weighted mean age of 158.8 ± 2.4 Ma (MSWD = 2.4, n = 11) (Fig. 9a). Fourteen analyses of the zircons grains from JD004 show $^{206}Pb/^{238}U$ ages varying from 153.7 ± 2.8 to 164.5 ± 2.5 Ma and a weighted mean age of 158.3 ± 1.9 Ma (MSWD = 1.7, n = 14) for JDB004 (Fig. 9b). Thirteen analyses of the zircons from JDB006 yield $^{206}Pb/^{238}U$ ages varying from 155.5 ± 2.4 to 167.7 ± 2.5 Ma, with a weighted mean age of 160.6 ± 2.1 Ma (MSWD = 2.5, n = 13) (Fig. 9c).

6.2. Molybdenite Re–Os age

The Re, Os contents and isotopic values of six molybdenite samples from the Linghou polymetallic deposit are listed in Table 2. Total Re and ^{187}Os concentrations vary from 195.4 to 226.3 ppb and 335.4 to 384.1 ppb, respectively. The Re–Os model ages of six molybdenite samples vary from 160.3 ± 2.1 to 164.1 ± 2.3 Ma, with a weighted average age of 162.2 ± 1.4 Ma (2σ, MSWD = 1.4) (Fig. 10). Our measured age of 221.4 ± 5.6 Ma for the molybdenite standard GBW04435 is consistent with the certified value of 220.6 ± 3.2 Ma within error limits and the Re and Os contents of six molybdenite samples are undistinguished in Table 2, indicating that the molybdenite Re–Os isotopic data in this analysis is credible.

6.3. Muscovite Ar–Ar age

The Ar–Ar isotopic data of muscovite (JDB101) is given in Table 3 and illustrated in Fig. 11. The results yield a well-defined plateau age of 155.7 ± 1.1 Ma (Fig. 11a), a normal and inverse isochron age of 160.2 ± 1.1 Ma (Fig. 11b) and 160.2 ± 1.1 Ma, respectively (Fig. 11c). The initial $^{40}Ar/^{36}Ar$ values are 46.5 ± 42.6 and 46.5 ± 17.8 Ma, respectively.

7. Discussion

7.1. Timing of the magmatic and mineralization events in the Linghou mining area

Early feldspar and whole rock K–Ar dating indicated that the granodiorite phases in the Linghou ore district have formed at

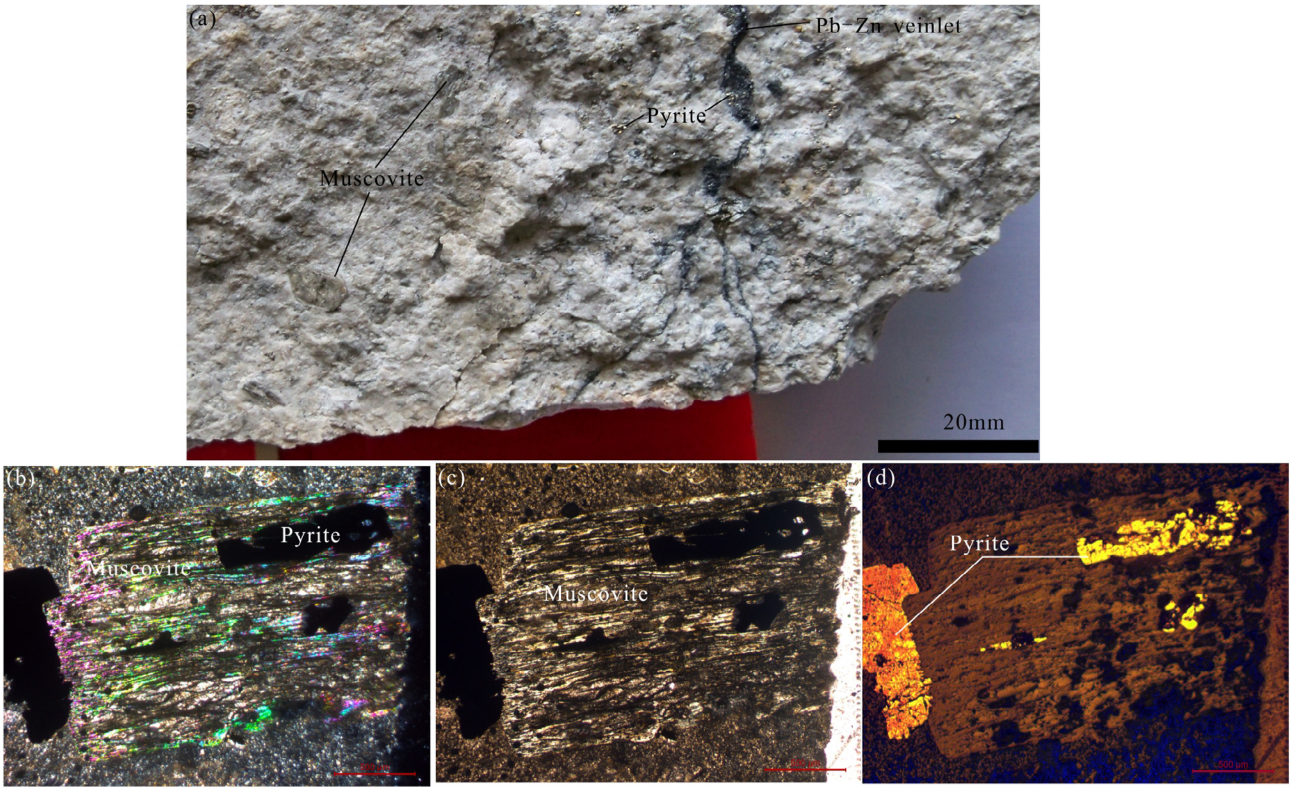

Fig. 6. Hydrothermal muscovite in the altered granodiorite porphyry (phase 2). (a) Altered granodiorite porphyry (phase 2) with disseminated pyrite and galena-sphalerite-pyrite veinlet; (b–d) Pyrite occurred in or near the muscovite in cross-polarized light (b), the polarized light (c) and reflected light (d).

the Cretaceous (115–122 Ma) (Zhou and Yu, 1983). However, such ages are completely unreliable as these granodiorite porphyries were extensively altered during which the K–Ar system was intensively modified (Fitch et al., 1969; Yamasaki et al., 2011; Clauer, 2013). Recently, Jia et al. (2014) reported a zircon LA–MC–ICP–M S U–Pb age of 169.9 ± 1.4 Ma for the biotite granodiorite porphyry, but did not provide the ages for other granodiorite porphyry phases. In this study, our new zircon U–Pb dating provide tight constrains on the ages of the biotite granodiorite porphyry (158.8 ± 2.4 Ma), granodiorite porphyry (phase 1) (158.3 ± 1.9 Ma) and granodiorite porphyry (phase 2) (160.6 ± 2.1 Ma). These new ages dataset clearly indicate that three granodiorite porphyries have formed at a very limited interval (158.3–160.6 Ma). It is noteworthy that the obtained age of 158.8 ± 2.4 Ma for the biotite granodiorite porphyry is much younger than that (169.9 ± 1.4 Ma) obtained by Jia et al. (2014). We consider that such a difference is due to two different dating methods as the uncertainty of LA–(MC)–ICP–MS is up to ±4% (2RSD) (Li et al., 2015).

L. Chen et al. (2013) reported Re–Os ages of ~122 Ma for the pyrrhotite in the Linghou deposit. However, this study did not provide the textural relationship of the pyrrhotite with Cu mineralization. Indeed, our study indicates that the pyrrhotite may have been present in late pyrrhotite–pyrite mineralization event that overprints the Cu mineralization. In current study, six molybdenite samples, which are intergrown with chalcopyrite, pyrite and quartz (Fig. 7), are collected in the copper mining tunnel near the Cu–Au–Ag ore bodies. Therefore, molybdenite is believed to be simultaneous with other metallic minerals in Cu–Au–Ag ore bodies, and its Re–Os age could represent the formation age of the Cu–Au–Ag mineralization. All the molybdenite samples give the model ages between 160.3 and 164.1 Ma and a weighted average age of 162.2 ± 1.4 Ma, which is clearly much older than the Re-Os ages of pyrrhotite obtained by L. Chen et al. (2013).

It was confirmed that the biotite could be altered to muscovite when it experienced intensive hydrothermal alteration (Borodina and Fershtater, 1988; Zhang et al., 2010). The granodiorite porphyry (phase 2) was extensively altered and mineralized, characterized by occurrence of disseminated pyrite and the galena–sphalerite–pyrite vein. In these altered rocks, muscovite was intergrown with pyrite (Fig. 6), and thus is believed to be hydrothermal in origin and related to Pb–Zn–Cu mineralization. The closure temperature of Ar isotope system in muscovite is about 350 ± 50 °C (Chen et al., 2011a), which is consistent with the formation temperature of the Pb–Zn–Cu ore bodies (350–480 °C, Tang et al., 2015b). The eight continuous steps at temperatures of 600–1030 °C are relatively coincident, and constitute a uniform and remarkably flat $^{40}Ar/^{39}Ar$ age spectra with 85.2% ^{39}Ar released. However, the initial $^{40}Ar/^{36}Ar$ ratios of 46.5 ± 42.6 Ma or 48.3 ± 17.8 Ma are obviously less than the atmospheric value of 298.56 ± 0.31 Ma (Lee et al., 2006), indicating that there was likely the loss of small quantities of ^{40}Ar (Hanson et al., 1975; Chen et al., 2011a). In this situation, the isochron method can also give a reliable age (Chen et al., 2011a). Therefore, the Ar–Ar isochron age of 160.2 ± 1.1 Ma is more reliable and represents the age of the late Pb–Zn–Cu mineralization event in the Linghou polymetallic deposit.

7.2. Origin of the Linghou polymetallic deposit

On the basis of the close relationships between the orebodies and granodiorite porphyries, as well as the characteristics of alteration and mineralization, Xu et al. (1981) and Zhou and Yu (1983)

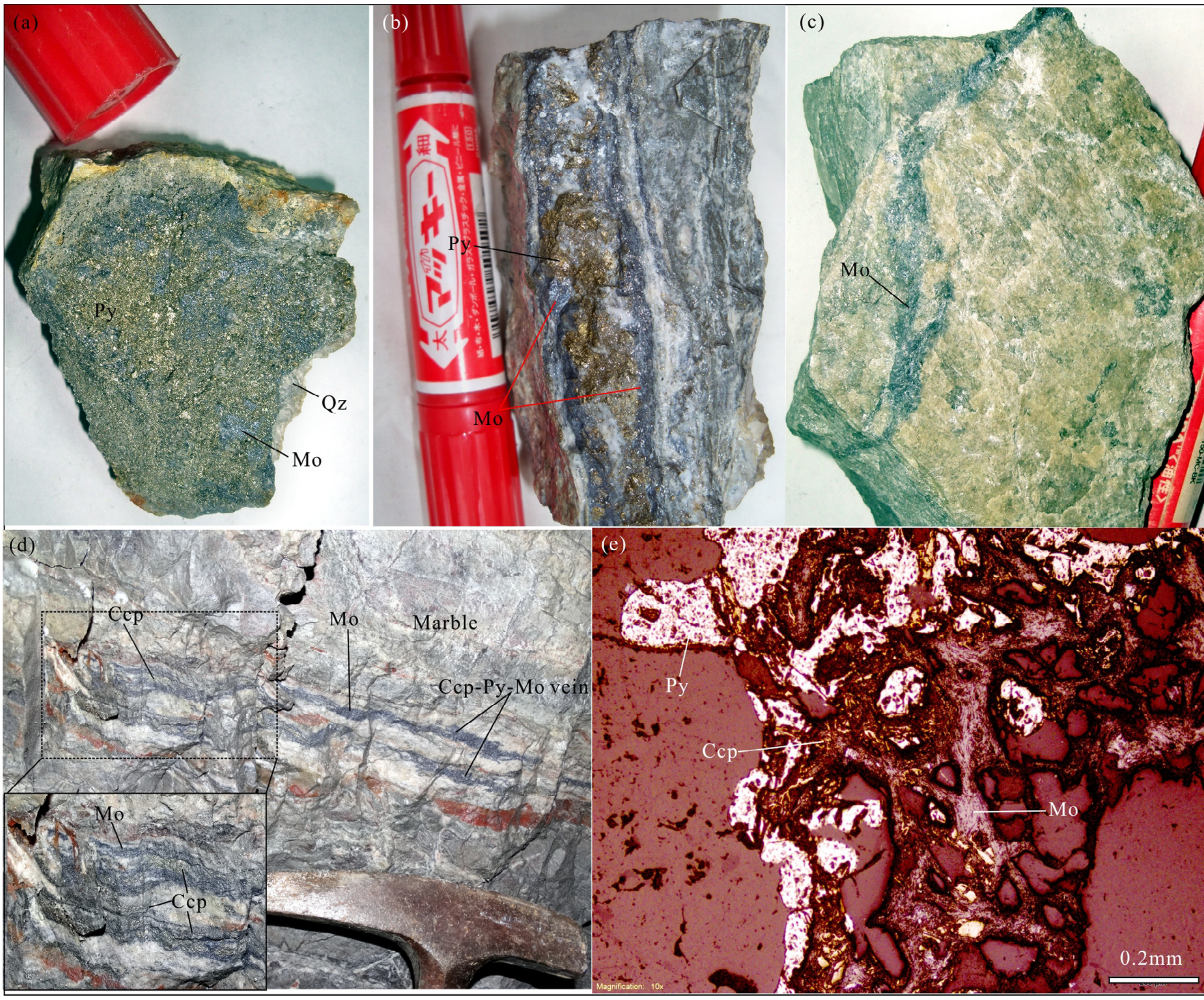

Fig. 7. Photographs and microphotos of molybdenite vein or veinlets in the Linghou deposit. (a) Py–Qz–Mo vein from the fracture; (b) Py–Qz–Ccp–Mo vein in marble; (c) Mo vein in fine sandstone and shale; (d) Py–Qz–Ccp–Mo veinlet occurred in "stratiform" or laminated shape in marble; (e) microphotos of Py–Qz–Ccp–Mo veins in marble; Py–Pyrite, Ccp–chalcopyrite, Qz–quartz, Mo–molybdenite.

classified this deposit into a skarn type deposit. Wang (1990) further indicated that this deposit was controlled by the magmatic, strata and structure. Alternatively, Cao et al. (1988) and Liu et al. (1996) considered that it should be a SEDEX-type deposit, based on following lines of evidence: (1) presences of the "stratiform" orebodies, and the laminate and crumpled textures of the ores; (2) some fluid inclusions have mid-low temperatures (from 154 to 286 °C) and low salinities (~5.3 wt.% NaCl eqv.); (3) the δ^{34}S values vary from −0.30‰ to +4.42‰; (4) galena and pyrite have the Pb isotopic model ages from 309 to 461 Ma; (5) the enrichment regularity of Cu, Pb, Zn and trace elements of pyrite. Indeed, based on the laminate and crumpled textures for the sulfides and the Re–Os isochron ages of the pyrrhotites, L. Chen et al. (2013) proposed that the Linghou deposit should be a SEDEX-type deposit which modified by a late magmatic-hydrothermal activity. However, recent studies shows that the typical SEDEX-type deposits are commonly characterized by syngenetic textures of ore bodies with similar ages to host rocks, a principal origin of evaporated seawater/basinal brines for the ore fluids with temperatures <300 °C and salinities >10% NaCl eqv., a principal origin of seawater and sedimentary sulfate for sulfur and the crustal sources for ore metals (Leach et al., 2005, 2010). Moreover, more and more cathodoluminescence (CL) imaging and new dating methods confirmed that the so-called "syngenetic" textures are not always reliable. For example, according to our dating results, the molybdenite–chalcopyrite–pyrite laminates in Fig. 7d cannot be syngenetic but metasomatic textures that are commonly present in skarn and other replacement-type deposits (e.g., Quartz–calcite–sulfides selectively replace some bands of garnet and fill the interstices; Chang and Meinert, 2008). On the other hand, these that more than half of equilibrium temperatures are over 300 °C (315 °C, 331 °C and 339 °C) and the sanities are also too low (<10% NaCl eqv.) (Cao et al., 1988), are also not consistent with a SEDEX origin. A narrow range of δ^{34}S values are not the supportive evidence for a SEDEX origin, as such values are common in many magmatic systems (−3‰ to +7‰, Ohmoto and Goldhaber, 1997). Finally, the Pb model ages have long been considered to be unreliable, and thus cannot be simply used to constrain the ages of deposits (Zhang and Zhang, 2009). Additionally, enrichment regularity of Cu, Pb, Zn and trace elements of pyrite are rarely used to identify the SEDEX-type deposit (see Leach et al., 2005, 2010 and the related references).

Table 1
Zircon U–Pb dating results of three granodiorite porphyry phases in the Linghou polymetallic deposit.

Spot	Pb	^{232}Th	^{238}U	Th/U	Isotopic ratios						Age (Ma)			
	ppm				$^{206}Pb/^{238}U$	1σ (%)	$^{208}Pb/^{232}Th$	1σ (%)	$^{207}Pb/^{206}Pb$	1σ (%)	$^{208}Pb/^{232}Th$	1σ (%)	$^{206}Pb/^{238}U$	1σ (%)
Biotite granodiorite porphyry (JDB021)														
11	13	297	423	0.70	0.0245	1.20	0.0078	1.90	0.0511	2.80	157.4	3.0	155.6	1.9
12	9	133	334	0.40	0.0259	1.50	0.0083	2.50	0.0529	3.70	166.2	4.1	163.8	2.5
13	8	135	285	0.47	0.0243	1.30	0.0082	2.30	0.0562	2.80	165.7	3.8	153.4	2.1
14	6	82	216	0.38	0.0252	1.60	0.0075	2.90	0.0518	4.10	150.9	4.4	160.1	2.5
15	9	178	320	0.56	0.0251	1.30	0.0081	2.00	0.0497	2.90	163.6	3.3	159.9	2.0
17	7	87	258	0.34	0.0252	1.80	0.0121	3.20	0.0693	4.10	244.0	7.8	156.5	2.8
18	5	88	175	0.50	0.0256	1.50	0.0081	2.90	0.0552	4.20	163.8	4.7	161.8	2.5
19	7	140	259	0.54	0.0252	1.40	0.0077	2.30	0.0477	3.60	156.0	3.6	160.3	2.2
20	3	56	141	0.40	0.0258	1.70	0.0085	3.40	0.0482	5.10	171.9	5.8	164.2	2.7
22	8	125	288	0.43	0.0246	1.30	0.0081	2.40	0.0537	3.50	163.4	4.0	155.5	2.0
24	5	56	206	0.27	0.0253	1.60	0.0081	3.20	0.0502	3.90	162.2	5.3	161.2	2.6
Granodiorite porphyry (phase 1, JDB004)														
44	8	133	287	0.46	0.0256	1.30	0.0077	2.30	0.0496	2.90	155.1	3.6	162.9	2.1
45	8	92	263	0.35	0.0258	1.50	0.0083	2.60	0.0485	3.40	167.0	4.4	164.5	2.5
46	8	178	249	0.71	0.0252	1.50	0.0078	2.60	0.051	3.70	156.7	4.0	159.9	2.3
47	9	192	281	0.68	0.0254	1.30	0.0094	2.00	0.066	2.70	189.7	3.8	158.5	2.1
48	7	86	168	0.51	0.027	1.50	0.0189	2.40	0.1297	2.80	378.8	9.0	154.7	2.4
50	7	98	256	0.38	0.0253	1.40	0.0079	2.70	0.051	3.70	159.1	4.3	160.6	2.2
51	11	264	373	0.71	0.0244	1.20	0.0077	1.90	0.048	3.20	155.8	3.0	155.2	1.9
52	7	75	234	0.32	0.0243	3.20	0.0074	6.50	0.0535	7.40	148.6	9.7	153.7	5.0
53	2	2	93	0.02	0.0251	3.80	0.0043	80.80	0.0501	12.20	87.0	70.3	159.8	6.2
54	7	76	151	0.51	0.0285	1.70	0.0234	2.50	0.1592	2.60	468.0	11.9	156.3	2.8
55	8	70	185	0.38	0.0282	1.60	0.0266	2.10	0.1526	2.90	530.0	11.4	156.2	2.7
56	7	85	194	0.44	0.0266	1.80	0.0215	2.90	0.122	3.00	430.3	12.4	153.7	2.8
57	7	126	233	0.54	0.025	1.50	0.0077	2.50	0.0555	3.90	154.8	3.9	157.9	2.4
58	11	145	258	0.56	0.0288	1.80	0.0221	2.80	0.1575	3.00	441.5	12.4	158.5	3.0
Granodiorite porphyry (phase 2, JDB006)														
26	7	98	228	0.43	0.0264	1.50	0.0088	2.70	0.0501	3.20	177.4	4.7	167.7	2.5
27	10	206	320	0.65	0.0250	1.30	0.0077	2.10	0.0541	3.00	155.0	3.3	158.0	2.0
28	7	122	220	0.56	0.0261	1.60	0.0081	2.40	0.0472	3.50	162.8	3.9	166.1	2.6
29	9	131	296	0.44	0.0253	1.40	0.0081	2.20	0.0487	3.10	163.6	3.6	161.2	2.3
31	7	102	240	0.42	0.0245	1.50	0.0078	2.70	0.0525	3.70	156.2	4.2	155.5	2.4
32	7	128	215	0.59	0.0250	1.60	0.008	2.20	0.052	3.80	162.0	3.6	158.9	2.6
34	11	265	333	0.79	0.0253	1.30	0.0078	1.90	0.0467	3.60	156.7	3.0	161.2	2.2
35	8	108	295	0.37	0.0255	1.20	0.0078	2.70	0.0527	3.20	157.0	4.3	161.4	2.0
36	11	159	422	0.38	0.0247	1.30	0.0076	2.30	0.0493	3.20	152.5	3.4	157.5	2.0
37	9	164	306	0.54	0.0248	1.30	0.0079	2.30	0.0529	3.10	158.4	3.7	157.5	2.0
39	10	89	349	0.26	0.0260	1.20	0.009	2.70	0.0508	2.90	180.8	4.9	165.4	2.1
40	6	108	219	0.49	0.0250	1.50	0.0079	2.60	0.049	4.30	159.5	4.2	159.5	2.4
41	7	110	219	0.50	0.0252	1.60	0.0073	2.60	0.0519	4.10	146.7	3.8	159.7	2.5

In summary, although the syngenetic origin for some ores cannot fully excluded, our following geological and geochronological data well indicates that the Cu–Au–Ag and Pb–Zn–Cu mineralization in the Songkengwu ore field are dominantly magmatic-hydrothermal origin, and they have clear genetic relationship with granodiorite porphyries.

(1) **Evidence from geology:** It is well indicated that the Cu–Au–Ag and Pb–Zn–Cu ore bodies are spatially associated with the granodiorite porphyries. Most of ore bodies are directly in contact with the granodiorite porphyries (Fig. 4), and the contact zones of 5–10 cm thick consist mainly of detrital rocks from the intrusion in the form of transitional zone (Figs. 4a, c and d) and strike-slip surface (Fig. 4b). Locally, the Pb–Zn–Cu ores crosscut and entrap the granodiorite porphyry in the shape of "V" (Fig. 4d).

(2) **Evidence from geochronology:** Our new dating results well indicate that the timing of both the Cu–Au–Ag and Pb–Zn–Cu mineralization (~160 Ma) is undistinguishable from the granodiorite porphyries, but much younger than their host rocks (>299 Ma).

(3) **Evidence from previous fluid inclusions and isotopic data:** Early fluid inclusion studies show that the fluid inclusions in both the Cu–Au–Ag and Pb–Zn–Cu mineralization have high temperatures (from 300 to 470 °C and 350 to 480 °C, respectively) and mid-high salinities (from 7.70 to 21.68 wt.% NaCl eqv. and 8.66 to 12.55 wt.% NaCl eqv., respectively) (Tang et al., 2015a; H. Chen et al., 2016). Moreover, the fluids have calculated $\delta^{18}O_{H2O}$ and δD values from 5.54‰ to 13.11‰ and −71.8‰ to −105.1‰, respectively, consistent with a principally magmatic origin. The magmatic origin of the fluids is further supported by the $\delta^{13}C_{PDB}$ values (−2.78‰ to −4.63‰) of the calcite (Tang et al., 2015a). It is noteworthy that the sulfides in different ores of the deposit have a narrow $\delta^{34}S$ values from −1.42‰ to +4.30‰ and a homogeneous lead isotopic compositions with $^{206}Pb/^{204}Pb$ ranging from 17.958 to 18.587, $^{207}Pb/^{204}Pb$ ranging from 15.549 to 15.701, and $^{208}Pb/^{204}Pb$ ranging from 37.976 to 39.052, indicating that the sulfur was sourced from the magmatic system and the Pb was derived from a mixed source involving both mantle and crustal components (Tang et al., 2015a).

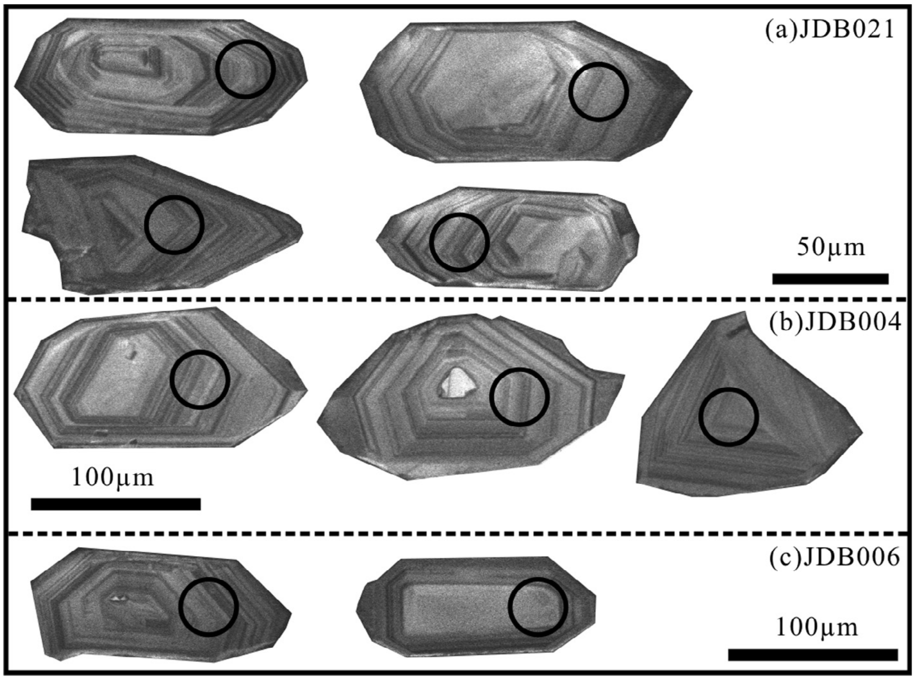

Fig. 8. Zircon cathodoluminescence images of three granodiorite porphyry phases in the Songkengwu ore field (with circles indicating the U–Pb dating positions).

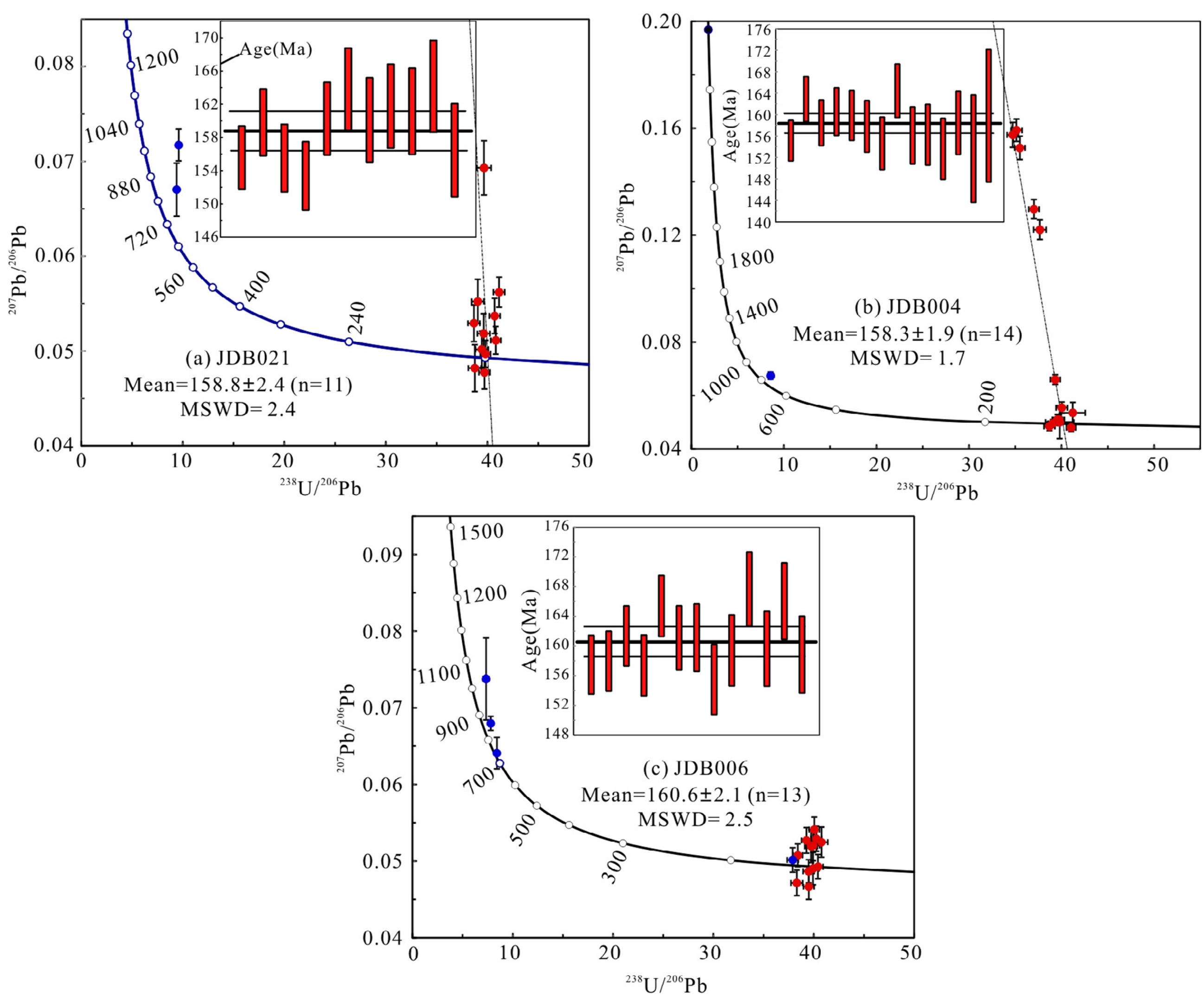

Fig. 9. Zircon U–Pb concordia diagrams of three granodiorite porphyry phases in the Songkengwu ore field.

Table 2
Re–Os isotopic data for molybdenite from the Linghou polymetallic deposit.

Sample	Weight (g)	Re (ppb)		Common Os (ppb)		^{187}Re (ppb)		^{187}Os (ppb)		Model age (Ma)	
		Measured	2σ	Measured	2σ	Measured	2σ	Measured	2σ	Measured	2σ
JDB051	0.00161	226.3	1.7	1.272	0.120	142.2	1.1	384.1	2.5	161.9	2.3
JDB0202	0.00107	222.8	1.5	1.526	0.347	140.0	0.9	374.4	2.3	160.3	2.1
JDB0202-2	0.00156	201.7	1.5	24.50	0.34	126.7	0.9	341.6	2.0	161.6	2.2
JDB0202-3	0.00116	212.7	1.8	204.8	1.5	133.7	1.1	362.5	2.8	162.6	2.4
JDB050	0.00167	196.2	1.7	11.43	4.12	123.3	1.1	335.4	2.9	163.0	2.5
JDB0122	0.00280	195.4	1.5	0.3156	0.1697	122.8	0.9	336.2	2.0	164.1	2.3

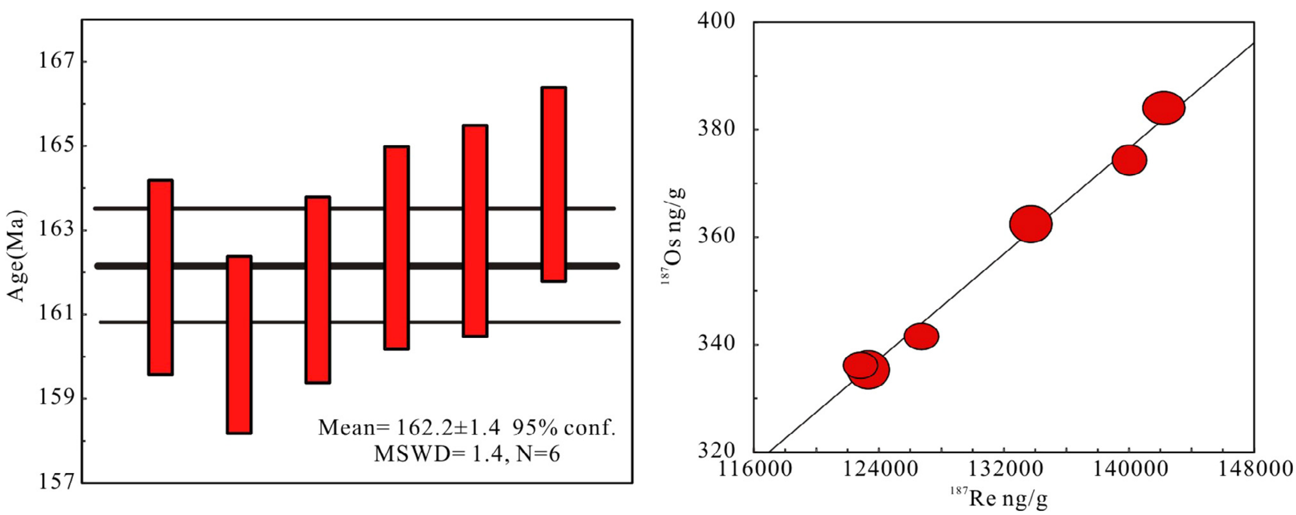

Fig. 10. Molybdenite Re–Os weighted mean model age and isochron plots in the Linghou polymetallic deposit.

Table 3
Results of $^{40}Ar/^{39}Ar$ stepwise heating analysis for muscovite from the Linghou polymetallic deposit.

T (°C)	$(^{40}Ar/^{39}Ar)_m$	$(^{36}Ar/^{39}Ar)_m$	$(^{37}Ar/^{39}Ar)_m$	^{40}Ar (%)	F	^{39}Ar ($\times10^{-14}$ mol)	^{39}Ar (%)	Age (Ma)	±1σ
Sample weight = 27.5 mg, J = 0.004378									
550	11.8479	0.0017	0.0041	95.68	11.3355	6.98	13.21	87.6	0.4
600	21.3204	0.0006	0.0060	99.10	21.1278	7.76	14.68	160.0	0.8
670	20.9790	0.0009	0.0049	98.71	20.7078	13.24	25.05	156.9	0.8
730	21.3348	0.0019	0.0057	97.30	20.7592	10.66	20.16	157.3	0.8
790	21.2101	0.0031	0.0063	95.68	20.2948	6.13	11.60	153.9	0.8
850	21.2968	0.0037	0.0089	94.92	20.2154	2.46	4.66	153.4	0.8
910	21.2670	0.0034	0.0091	95.32	20.2727	1.19	2.25	153.8	0.8
970	21.3734	0.0031	0.0100	95.67	20.4477	1.96	3.72	155.0	0.8
1030	21.4008	0.0030	0.0112	95.82	20.5062	1.63	3.08	155.5	0.8
1150	20.3207	0.0038	0.0414	94.46	19.1956	0.50	0.95	145.9	1.0
1250	19.9662	0.0064	0.0626	90.55	18.0805	0.35	0.65	137.8	1.1

F = $(^{40}Ar^{*}/^{39}Ar)$; m: the measured isotopic ratios.

(4) **Evidences from ore bodies and minerals:** Although they are relatively minor, skarn minerals and typical calc-silicate (skarn) alteration have really occurred in the Linghou deposit (Xu et al., 1981; Zhou and Yu, 1983). Garnets and chalcopyrite are present in the connect zone between the carbonate Formation and the Cu–Au–Ag ore bodies, although most of the garnets were replaced by chlorite, epidote and calcite (Fig. 3).

7.3. Implications for the metallogenesis, regional exploration and geological setting of the QHMB

Recently, more detailed geology, fluid inclusion, S–Pb–H–O isotopic and geochronological studies were available on the deposits in the QHMB (Table 4). The magmatic-hydrothermal system of the northeast QHMB is characterized by granitic complex (consists mainly of granodiorite and granite) and associated skarn and porphyry deposits, including the 140–160 Ma Linghou skarn and carbonate-replacement types Cu–Au–Ag and Pb–Zn–Cu polymetallic (Tang et al., 2015a), Tongcun porphyry-skarn type Mo–Cu (Tang et al., 2015b), Lizhu skarn type Fe–Zn–Mo (Zhang et al., 2015), Yinshan skarn type Ag–Pb–Zn polymetallic (He et al., 2011) and Anji skarn-porphyry type Fe–Zn–Pb–Cu polymetallic deposits (Xie et al., 2012a) (Fig. 1 and Table 4). Moreover, several previously considered "SEDEX" type deposits, which is similar to the Linghou deposit, are also confirmed to be magmatic-hydrothermal origin (Table 4), including the Yongping porphyry-skarn Cu–Mo (Li et al., 2013a), Dongxiang porphyry? Cu (Cai et al., 2011), Shuikoushan (Kangjiawan) skarn Pb–Zn (Lu et al., 2013; Zuo et al., 2014; Huang et al., 2015), Fozichong skarn Pb–Zn (Fu et al.,

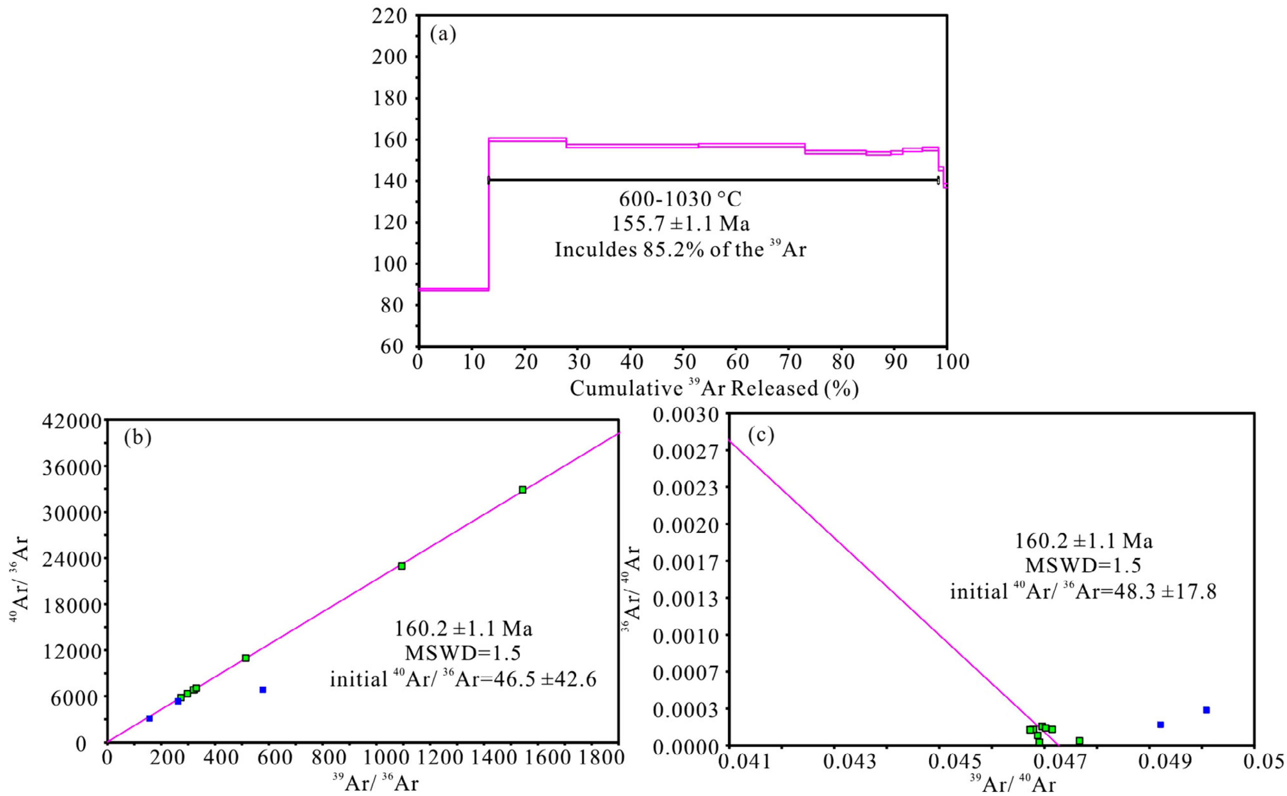

Fig. 11. Stepwise laser ablation analytical $^{39}Ar/^{40}Ar$ data for muscovite. (a) Plateau age; (b) normal isochron age; (c) inverse isochron age.

2013) and Dabaoshan porphyry-skarn Mo–Cu–Pb–Zn deposits (Wang et al., 2012a; Mao, 2016). Other deposits, including Tieshajie Cu (Luo, 2010; Wang et al., 2013a,b), Yunfu and Dajiangping pyrite deposits (Chen et al., 1998; Zhao et al., 2016), are also confirmed to be modified by the late magmatic-hydrothermal activities. All these above suggest that the SEDEX-type deposits in the QHMB are not as important as the previous scholars thought, whereas the magmatic-hydrothermal and mineralization events in middle-late Jurassic period (about 140–160 Ma) have been playing the dominant role in this belt. Actually, based on the SEDEX-type model in exploration, there have few new deposits been found in the past three decades (see the deposits introduction in Mao et al., 2011a and Xu et al., 2012, 2015). However, recent exploration activities have confirmed and reported some large magmatic-hydrothermal deposits, such as the Yuanzhuding porphyry Cu–Mo (Zhong et al., 2010, 2013), Shedong porphyry–skarn–quartz vein type (Chen et al., 2011b), Gaocheng Pb–Zn–Ag (Zhao et al., 2012) and Xitian skarn-vein type W–Sn deposits (Y. Zhou et al., 2015). Therefore, we suggest that magmatic-hydrothermal type deposits (e.g., porphyry and skarn types) can be the most important targets for exploration in the QHMB.

In the previous studies, the Linghou as well as other previously-considered ''SEDEX'' type deposits was suggested to have formed in a sag basin in continental rifts setting during the Silurian and Triassic period (Cao et al., 1988; Xu et al., 1996; Liu et al., 1996; Gu et al., 2003). Such an interpretation is clearly not supported by new dating results, which suggest that these deposits have mainly formed in 150–160 Ma (Table 4). Considering that the Southeastern China was controlled in the Paleo-Pacific tectonic regime at that time, it is proposed that these deposits formed in the subduction-related setting (Mao et al., 2011a).

8. Conclusions

Granodiorite porphyries from the Songkengwu ore field have zircon U-Pb ages of ~160 Ma. Such ages are comparable to newly obtained molybdenite Re–Os age of 162.2 ± 1.4 Ma for the Cu–Au–Ag mineralization and muscovite Ar–Ar age of 160.2 ± 1.1 Ma for the late Pb–Zn–Cu mineralization. The Cu–Au–Ag and Pb–Zn–Cu mineralization in the Songkengwu ore field have the genetic relationship with these intrusions and thus should be magmatic-hydrothermal in origin. This study thus confirmed that the Linghou and other similar polymetallic deposits in the QHMB cannot be ''SEDEX'' type as previously considered. Instead, these deposits have mainly formed in a subduction-related setting in middle-late Jurassic period. This study also highlights that the intrusion-related deposits (e.g., porphyry and skarn types) in 140–160 Ma could be the most important targets for exploration in the QHMB.

Acknowledgments

This study was financially supported by the National Natural Science Foundation of China (Grant No. 41602093), the DREAM project of MOST China (2016YFC0600405) and 12th Five-Year Plan Project of State Key Laboratory of Ore-deposit Geochemistry, Chinese Academy of Sciences (SKLODG-ZY125-xx). We are grateful to Editor-in Chief Dr. Meifu Zhou, Guest Editor Dr. Wei Terry Chen

Table 4
The ages of intrusive rocks and associated mineralization in the QHMB.

Ore deposit	Metal association and deposit type	Related intrusion	Previous evidences for SEDEX	New evidences for magmatic-hydrothermal origin			Reference
				Timing of intrusion (Ma)	Associated mineralization age (Ma)	Other evidences	
Deposits in the northeast QHMB							
Linghou polymetallic deposit	Cu–Au–Ag and Pb–Zn–Cu Skarn	Complex (granodiorites)	See the text in Section 7.2	Zircon LA–ICP–MS U–Pb 158.3 ± 1.9–160.6 ± 2.1	162.2 ± 1.4, 160.2 ± 1.1	See the text in Section 7.2	This paper
Tongcun deposit	Mo–Cu, little Pb–Zn Porphyry-skarn	Complex (granodiorite, granites)	None	Zircon LA–ICP–MS U–Pb 162.1 ± 3.4	Molybdenite Re–Os 162.2 ± 1.3–163.0 ± 2.4	–	Zhu et al., 2014; Zhang et al., 2013; Tang et al., 2015b
Lizu deposit	Fe–Zn–Mo Skarn	Complex (granite and granodiorite)	None	Zircon LA–ICP–MS U–Pb 147.2 ± 1.7–162.4 ± 0.9	Molybdenite Re–Os 150.7 ± 1.6	–	Gu et al., 2011; Jia et al., 2014; Zhang et al., 2015
Anji polymetallic deposit	Fe–Zn–Cu, Pb–Zn–Ag–Cu, and Mo Skarn-porphyry	Complex (granites and granoirite)	None	Zircon LA–ICP–MS U–Pb 150.2 ± 1.3–139.2 ± 1.2 (Certified by 91500)	Molybdenite Re–Os 139 ± 5	–	Xie et al., 2012a,b; Tang et al., 2012, 2013
Mugua	W–Mo	Granite porphyry	None	No report		–	Li et al., 2013b
Zhuxiling	W–Mo Skarn-porphyry	Granite	None	Zircon LA–ICP–MS U–Pb 138 ± 1.3–142.4 ± 1.6	No report	–	X.F. Chen et al., 2013
Deposits in the middle and southwest QHMB							
Yongping	Cu–Mo–W Porphyry-skarn	Dacite, porphyry and quartz porphyry	Stratiform orebodies and the laminate textures of the ores; Th: 180–360 °C, *w*(NaCl) eq: 2.5–4.5%; δ^{34}S: 0.4‰ to +4.3‰; Lead isotopes: ^{206}Pb/^{204}Pb = 17.494–18.239, ^{207}Pb/^{204}Pb = 15.387–15.751, ^{208}Pb/^{204}Pb = 37.595–39.159 and Pb model ages of 330–609 Ma	Zircon SHRIMP U–Pb 156–162	Molybdenite Re–Os 156	Porphyry and skarn alteration; Th: 212–486 °C, *w*(NaCl)eq: 7.4–10.3%; δ^{34}S‰: −0.2 to +1.9	Xu et al., 1998; Tian et al., 2001; Li et al., 2013a; J.J. Chen et al., 2016
Dongxiang	Cu Intrusion-related (porphyry?)	Granodiorite porphyry	Stratiform orebodies locally	Zircon SHRIMP U–Pb 156.4–161.0	Quartz Rb–Sr 161.8 ± 9.6	Th: 280–320 °C and 300–340 °C; *w*(NaCl)eq: 0.35–5.86% and 29.4–41.9%; δ^{34}S‰: −3.1 to +1.9; δ^{65}Cu‰: −2.012 to +0.136	Cai et al., 2011; Ou-Yang, 2015
Dabaoshan	Mo, Cu–Pb–Zn Porphyry-skarn	Granodiorite	Stratiform orebodies and banded structure for ores; Microfossils? in Py; Element zoning of Cu, Pb and Zn; Th = 148–320 °C, $\delta^{18}O_{H2O}$‰: −3.36 to +7.29; δ^{34}S for Po, Cp, Gn and Sp: −2.5‰ to +2.5‰; Lead isotopes (mean value): ^{206}Pb/^{204}Pb = 18.6303, ^{207}Pb/^{204}Pb = 15.6809, ^{208}Pb/^{204}Pb = 38.8226; Co/Ni values in Py and Po from 0.1 to 1.89	Zircon LA–ICP–MS U–Pb 162.2 ± 0.7	Molybdenite Re–Os 164.6 ± 0.9	Th: 280–410 °C and 174–355 °C; *w*(NaCl)eq: 3.7–14.7%; δ^{34}S: −4‰ to +5‰; Growth zoning of quartz associated with chalcopyrite in stratiform orebodies	Ge and Han, 1986; Wang, 2010; Mao, 2016
Shuikoushan Kangjiawang	Pb–Zn Skarn	Granodiorite	Stratiform orebodies	Zircon SIMS U–Pb 158.8 ± 1.8	Molybdenite Re–Os 157.8 ± 1.4	Th: 276–351 °C (vapor-rich); *w*(NaCl) eq: 2.6–4.5%; δ^{34}S: −2.71‰ to −0.90‰	Lu et al., 2013; Zuo et al., 2014; Huang et al., 2015
Fozichong	Pb–Zn–Cu Skarn	Granite porphyry?	Stratiform orebodies; Exhalative sedimentary rocks	Not clear	Sephalerite Rb–Sr 134.7 ± 3.5?	Th: 240–345°C; *w*(NaCl) eq: 3.5–5.4%; $\delta^{18}O_{H2O}$‰: 6.04 and 6.20, δD‰: −52.7 and −60.3; δ^{34}S: 2.3–4.3‰	Yang et al., 2000; Luo et al., 2012; Fu et al., 2013
Yunfu and Dajiangping	Py, Gn and Sp SEDEX and intrusion-related	Not clear	Exhalative sedimentary rocks; Stratiform and banded orebodies; Geochemistry of Py and host rocks; δ^{34}S: −10.9‰ to −25.6‰	Not clear	Sephalerite Rb–Sr 88.5 ± 3.9	Pb–Zn ore bodies were identified; Th: 220–400 °C; *w*(NaCl)eq: 6–9%; δ^{34}S: −7.1‰ to −6.4‰	Chen et al., 1998; Zhao et al., 2016

Table 4 (*continued*)

Ore deposit	Metal association and deposit type	Related intrusion	Previous evidences for SEDEX	New evidences for magmatic-hydrothermal origin: Timing of intrusion (Ma)	Associated mineralization age (Ma)	Other evidences	Reference
Tieshajie	Cu SEDEX or intrusion-related?	Not clear	Stratiform, banded and lenticular orebodies; Exhalative sedimentary rocks; $\delta^{34}S$: 3.0–5.9‰; Co/Ni values in Py: 0.63–1.43	Not clear	K-feldspar Ar–Ar 138.7 ± 2.7	$\delta^{34}S$: −4.3‰ to 6.3‰; Orogenic Pb characteristics in Cp: $^{206}Pb/^{204}Pb$ = 18.4138–18.4887, $^{207}Pb/^{204}Pb$ = 15.6021–15.6032, $^{208}Pb/^{204}Pb$ = 38.5596–38.6242	He et al., 2008; Luo, 2010; Wang et al., 2013b
Newly discovered deposits in the QHMB							
Yuanzhuding	Cu–Mo Porphyry	Granodiorite porphyry	None	Zircon LA-ICP-MS U–Pb 157.8 ± 1.1	Molybdenite Re–Os 155.6 ± 3.4–157.3 ± 4.3	–	Zhong et al., 2010, 2013
Xitian	W–Sn Skarn-vein type	Granite	None	Zircon LA-ICP-MS U–Pb 151.7 ± 1.2	Muscovite Ar–Ar 155.6 ± 1.7	–	Wang et al., 2015b; Y. Zhou et al., 2015
Shedong	W–Mo Porphyry–skarn–quartz vein type	Granodiorite porphyry	None	Zircon LA-ICP-MS U–Pb 435.8 ± 1.3	Molybdenite Re–Os 437.8 ± 3.4	–	Chen et al., 2011b
Gaocheng	Pb–Zn–Ag intrusion-related	Biotite granite?	None	Zircon LA-ICP-MS U–Pb 429 ± 13 Ma	Not clear	–	Zhao et al., 2012

Po–pyrrhotite, Py–Pyrite, Gn–galena, Sp–sphalerite, Cp–Chalcopyrite, "–" mean no need to give out.

and two anonymous reviewers for their constructive reviews and significant help in improving the original manuscript.

References

Baker, J., Peate, D., Waight, T., Meyzen, C., 2004. Pb isotopic analysis of standards and samples using a $^{207}Pb–^{204}Pb$ double spike and thallium to correct for mass bias with a double-focusing MC–ICP–MS. Chem. Geol. 211 (3–4), 275–303.

Black, L.P., Kamo, S.L., Allen, C.M., Aleinikoff, J.N., Davis, D.W., Korsch, R.J., Foudoulis, C., 2004. TEMORA 1: a new zircon standard for Phanerozoic U-Pb geochronology. Chem. Geol. 200 (1–2), 155–170.

Borodina, N.S., Fershtater, G.B., 1988. Composition and nature of muscovite in granites. Int. Geol. Rev. 30, 375–381.

Bureau of Geology and Mineral Resources of Zhejiang Province (BGMRZP), 1989. Regional geology of Zhejiang Province. People's Republic of China, Ministry of Geology and Mineral Resources. Geological Memoirs, Series 1, No. 11. Geological Publishing House, Beijing, pp. 519–526 (in Chinese with English abstract).

Cai, Y.T., Ni, P., Shen, K., Zhu, X.T., Huang, S.J., Zhang, X.C., Xu, J.H., 2011. Study on the fluid inclusion from Dongxiang copper deposit, Jiangxi Province, China. Acta Petrol. Sin. 27 (5), 1375–1386 (in Chinese with English abstract).

Cao, S.Y., Liu, J.J., Li, Y.L., 1988. Geologic characteristics and the metallogenetic model of submarine volcanic hydrothermal sedimentary mineralization of the polymetallic deposit in Linghou, Zhejiang province, China. J. Chengdu Inst. Geol. 15, 11–20 (in Chinese with English abstract).

Chang, Z.S., Meinert, L., 2008. The empire Cu-Zn mine, Idaho, USA: exploration implications of unusual skarn features related to high fluorine activity. Econ. Geol. 103, 909–938.

Chen, B.S., 2005. The Geological Survey Report of Songkengwu Ore Field (No. 33–30 lines) in Jiande Copper Deposit, Zhejiang Province. Zhejiang Institute of Geology and Mineral Exploration for Non-ferrous Metals, pp. 5–6 (in Chinese).

Chen, B., Zhou, X.X., 2012. Ore-controlling factors and a metallogenic model for the Xianglushan Tungsten-ore field in northern Jiangxi Province. Geol. Explor. 48, 0562–0569 (in Chinese with English abstract).

Chen, D.F., Chen, G.Q., Pan, J.M., Ma, S.G., Dong, W.Q., Gao, J.Y., Chen, X.P., 1998. Characteristics of the hydrothermal sedimentation of the Dajiangping superlarge pyrite deposit in Yunfu. Guangdong. Geochim. 27 (1), 12–19 (in Chinese with English abstract).

Chen, W., Wan, Y.S., Li, H.Q., Zhang, Z.Q., Dai, T.M., Shi, Z.E., Sun, J.B., 2011a. Isotope geochronology: technique and application. Acta Geol. Sin. 85 (11), 1917–1947 (in Chinese with English abstract).

Chen, M.H., Mo, C.S., Huang, Z.Z., Li, B., Huang, H.W., 2011b. Zircon LA–ICP–MS U-Pb ages of granitoid rocks and molybdenite Re–Os age of Shedong W–Mo deposit in Cangwu County of Guangxi and its geological significance. Miner. Depos. 30 (6), 963–978 (in Chinese with English abstract).

Chen, X.F., Wang, Y.G., Sun, W.D., Yang, X.Y., 2013. Zircon U-Pb chronology, geochemistry and genesis of the Zhuxiling granite in Ningguo, Southern Anhui. Acta Geol. Sin. 87 (11), 1662–1678 (in Chinese with English abstract).

Chen, L., Wang, Z.Q., Zhao, Y.Y., Liu, Y., Cao, J., Ding, L., Qu, W.J., 2013. Re–Os isotopic dating of pyrrhotite in the Linghou Cu deposit, Jiande, Zhejiang province and its geological significance. Acta Geol. Sin. 87 (12), 1864–1873 (in Chinese with English abstract).

Chen, H., Ni, P., Chen, R.Y., Ye, T.Z., Wang, G.G., Zhang, B.S., Xu, Y.F., 2016. Fluid inclusion studies of the jiande copper deposit, Zhejiang Province, China. Geol. J. China Univ. 22 (1), 001–011 (in Chinese with English abstract).

Chen, J.J., Cao, D.H., Yang, X.L., Qiu, C.R., Wang, X.J., Kan, Y.S., 2016. Fluid inclusions and sulfur isotope of the Yongping copper-polymetallic deposit in Jiangxi Province. Acta Geosci. Sin. 37, 163–173 (in Chinese with English abstract).

Clauer, N., 2013. The K-Ar and $^{40}Ar/^{39}Ar$ methods revisited for dating fine-grained K-bearing clay minerals. Chem. Geol. 354, 163–185.

Dong, S.W., Zhang, Y.Q., Long, C.X., Yang, Z.Y., Ji, Q., Wang, T., Hu, J.M., Chen, X.H., 2008. Jurassic tectonic revolution in China and new interpretation of the Yanshan movement. Acta Geol. Sin. (Engl. Ed.) 82 (2), 334–347.

Du, A.D., He, H.Y., Yin, W.N., Zhou, X.Q., Sun, Y.L., Sun, D.Z., Chen, S.Z., Qu, W.J., 1994. The study on the analytical methods of Re–Os age for molybdenites. Acta Geol. Sin. 68, 339–347 (in Chinese with English abstract).

Du, A.D., Wu, S.Q., Sun, D.Z., Wang, S.X., Qu, W.J., Markey, R., Stain, H., Morgan, J., Malinovskiy, D., 2004. Preparation and certification of Re–Os dating reference materials: molybdenite HLP and JDC. Geostand. Geoanal. Res. 28 (1), 41–52.

Feng, C.Y., Zhang, D.Q., Xiang, X.K., Li, D.X., Qu, H.Y., Liu, J.N., Xiao, Y., 2012. Re–Os isotopic dating of molybdenite from the Dahutang tungsten deposit in northwestern Jiangxi Province and its geological implication. Acta Petrol. Sin. 28 (12), 3858–3868 (in Chinese with English abstract).

Fitch, F.J., Miller, J.A., Mitchell, J.G., 1969. A new approach to radio-isotopic dating in orogenic belts. In: Kent, P.E., Sattherthwaite, G.E., Spencer, A.M. (Eds.), Time and Place in Orogeny, vol. 3. Geological Society, London, Special Publications, pp. 157–195.

Fu, W., Chai, M.C., Yang, Q.J., Wei, L.M., Huang, X.R., Feng, J.P., 2013. Genesis of the Fozichong Pb–Zn polymetallic deposit: constraints from fluid inclusions and H-O–S–Pb isotopic evidences. Acta Petrol. Sin. 29 (12), 4136–4150 (in Chinese with English abstract).

Ge, C.H., Han, F., 1986. Submarine volcanic hydrothermal sedimentary origin of the Dabaoshan iron and polymetallic sulfide deposit. Miner. Depos. 5 (1), 1–12 (in Chinese with English abstract).

Gu, L.X., Hu, W.X., Ni, P., He, J.X., Xu, Y.T., Lu, J.J., Lin, C.M., Li, W.Q., 2003. New discussion on the south China-type massive sulphide deposits formed on continental crust. Geol. J. China Univ. 9 (4), 592–608 (in Chinese with English abstract).

Gu, M.G., Feng, L.X., Hu, Y.H., Yu, S.Q., Wu, M., 2011. LA–ICP–MS U-Pb dating of zircons from Guangshan and Zhaxi plutons in Shaoxing area, Zhejiang Province: constraint on the ore-forming epoch of the Lizhu iron ore deposit. Geol. Bull. China 30 (8), 1212–1219 (in Chinese with English abstract).

Guo, S., Zhao, Y.Y., Qu, H.C., Wu, D.X., Xu, H., Li, C., Liu, Y., Zhu, X.Y., Wang, Z.K., 2012. Geological characteristics and ore-forming time of the Dexing porphyry copper ore mine in Jiangxi province. Acta Geol. Sin. (Engl. Ed.) 86, 691–899.

Hanson, G.N., Simmons, K.R., Bence, A.E., 1975. $^{40}Ar/^{39}Ar$ spectrum ages for biotite, hornblende and muscovite in a contact metamorphic zone. Geochim. Cosmochim. 39, 1269–1278.

He, J.R., Wang, A.G., Rui, X.J., Li, C.H., 2005. Discussion on mineralizing process in east integrating zone of Qinzhou Bay and Hangzhou Bay: in Earth science technology forum of six provinces and one municipality in East China, 2005 in Nanjing, Jiangsu province, China. Jiangsu Geol. Inst., 8–13 (in Chinese with English abstract)

He, J.R., Wang, A.G., Rui, X.J., Zhen, Y., Li, C.H., 2008. Middle Proterozoic submarine volcanic exhalative metallogenesis of Tieshajie, Yiyang, Jiangxi Province. Resour. Surv. Environ. 29 (4), 261–269 (in Chinese with English abstract).

He, G.J., Yang, X.C., Wu, G.M., Zhang, G.F., Cai, X.X., Zheng, J., 2011. A study of ore mineral characteristics and metallogenic stages of the Yinshan Ag–Pb–Zn polymetallic ore deposit, northwest Zhejiang province. Acta Geosci. Sin. 32, 304–312 (in Chinese with English abstract).

He, C.S., Santosh, M., Dong, S.W., 2015. Continental dynamics of Eastern China: insights from tectonic history and receiver function analysis. Earth-Sci. Rev. 145, 9–24.

Hong, D.W., Xie, X.L., Zhang, J.S., 2002. Geological significance of the Hangzhou–Zhuguangshan–Huashan high -ε_{Nd} granite belt. Geol. Bull. China 21 (6), 348–354 (in Chinese with English abstract).

Hua, R.M., Chen, P.R., Zhang, W.L., Lu, J.J., 2005. Three major metallogenic events in Mesozoic in South China. Miner. Depos. 24 (2), 291–304 (in Chinese with English abstract).

Huang, J.C., Peng, J.T., Yang, J.H., Zhang, B.L., Xu, C.X., 2015. Precise zircon U-Pb and molybdenite Re–Os dating of the Shuikoushan granodiorite-related Pb–Zn mineralization, southern Hunan. South China. Ore Geol. Rev. 71, 305–317.

Jackson, S.E., Pearson, N.J., Griffin, W.L., Belousova, E.A., 2004. The application of laser ablation-inductively coupled plasma-mass spectrometry to in situ U-Pb zircon geochronology. Chem. Geol. 211 (1–2), 47–69.

Jia, S.H., Zhao, Y.Y., Wang, Z.Q., Wu, Y.D., Wang, T., Chen, L., 2014. Zircon U-Pb dating and geochemical characteristics of granodiorite-porphyry in the Linghou copper deposit, Western Zhejiang, and their geological significance. Acta Geol. Sin. 11 (88), 2071–2089 (in Chinese with English abstract).

Leach, D.L., Sangster, D.F., Kelley, K.D., Large, R.R., Garven, G., Allen, C.R., Gutzmer, J., Walters, S., 2005. Sediment-hosted lead-zinc deposits: a global perspective. Econ. Geol. 100th anniversary volume, 561–608.

Leach, D.L., Bradley, D.C., Huston, D., Pisarevsky, S.A., Taylor, R.D., Gardoll, S.J., 2010. Sediment-hosted lead-zinc deposits in Earth history. Econ. Geol. 105 (3), 593–625.

Lee, J.Y., Marti, K., Severinghaus, J.P., Kawamura, K., Yoo, H.S., Lee, J.B., Kim, J.S., 2006. A redetermination of the isotopic abundances of atmospheric Ar. Geochim. Cosmochim. 70, 4507–4512.

Li, Y.G., 2000. Qiantang-Qingfang old plate junction zone and its geological significance. Geol. Zhejiang 16, 17–24 (in Chinese with English abstract).

Li, X.F., Xiao, R., Feng, Z.H., Wang, C.Y., Yang, F., Bai, Y.P., Jiang, S.K., Wang, Z.K., Zhu, X.Y., Xiao, N., Wei, X.L., 2011. Zircon SHRIMP U–Pb and biotite Ar–Ar ages from Fujiawu porphyry Cu–Mo deposit, Dexing, Southeast China: implications for magmatic-hydrothermal chronology. Let's Talk Ore Depos. I and II, 377–379.

Li, X.F., Hu, R.Z., Wei, X.L., Xiao, R., Xiao, N., Wang, C.Y., Yang, F., 2012. Mineral deposits types, mineralization features and genesis relationship between Jinshan gold deposit and Deixing porphyry copper deposit, northeastern Jiangxi province, South China. Geol. Rev. 58 (1), 82–90 (in Chinese with English abstract).

Li, X.F., Watanabe, Y., Yi, X.K., 2013a. Ages and sources of ore-related porphyries at Yongping Cu–Mo deposit in Jiangxi province, southeast China. Resour. Geol. 63, 288–312.

Li, Z.L., Zhou, J., Mao, J.R., Yu, M.G., Li, Y.Q., Hu, Y.Z., Wang, H.H., 2013b. Age and geochemistry of the granitic porphyry from the northwestern Zhejiang Province, SE China, and its geological significance. Acta Petrol. Sin. 29 (10), 3607–3622 (in Chinese with English abstract).

Li, X.H., Liu, X.M., Liu, Y.S., Su, L., Sun, W.D., Huang, H.Q., Yi, K., 2015. Accuracy of LA–ICP–MS zircon U-Pb age determination: an inter-laboratory comparison. Sci. China: Earth Sci. 58, 1722–1730.

Liu, J.J., Cao, S.Y., Li, Y.L., 1996. Origin of the Jiande copper deposit, Zhejiang. Miner. Resour. Geol. 53 (10), 145–154 (in Chinese with English abstract).

Lu, S.D., Gao, W.L., Wang, S.L., Xiao, E., Xu, J.H., Liu, J., 2005. Pb isotopic compositions and its significance for ore genesis in Zhangshiba Pb–Zn deposit, Jiangxi. J. Mineral. Petrol. 25, 64–69 (in Chinese with English abstract).

Lu, R., Xu, Z.W., Lu, J.J., Wang, R.C., Zuo, C.H., Zhao, Z.X., Miao, B.H., 2013. Genesis of the Shuikoushan lead-zinc deposit Changning City, Hunan Province. J. Nanjing Univ. (Nat. Sci.) 49 (6), 732–746 (in Chinese with English abstract).

Luo, P., 2010. Research on Metallogenic Regularities and Prospecting Orientation of Copper Polymetal Mineral Resources in the Northern Wuyi Region of Jiangxi Province. China Univ. Geosci., Beijing, pp. 94–96 (Paper for Doctoral Degree, in Chinese with English abstract).

Luo, J.H., Zhang, Y.H., Zhai, L.N., Liu, W., Jiang, H., 2012. The sphalerite Rb–Sr isotopic chronology of Fuzichong Pb–Zn deposit. Geol. Chem. Miner. 34 (1), 26–31 (in Chinese with English abstract).

Mao, W., 2016. Hydrothermal Fluid Evolution and the Ore-Forming Mechanism of the Dabaoshan Polymetallic Deposit, Guangdong Province, South China. Institute of Geochemistry, Chinese Academy of Sciences, pp. 1–140 (Paper for doctoral degree, in Chinese with English abstract).

Mao, J.R., Yutaka, T., Li, Z.L., Takahashi, N., Ye, H.M., Zhao, X.L., Zhou, J., Hu, Q., Zeng, Q.T., 2009. Correlation of Meso-Cenozoic tectono-magmatism between SE China and Japan. Geol. Bull. China 28 (7), 844–856 (in Chinese with English abstract).

Mao, J.W., Chen, M.H., Yuan, S.D., Guo, C.L., 2011a. Geological characteristics of the Qinhang (or Shihang) metallogenic belt in South China and spatial-temporal distribution regularity of mineral deposits. Acta Geol. Sin. 85 (5), 636–658 (in Chinese with English abstract).

Mao, J.W., Zhang, J.D., Pirajno, F., Ishiyama, D., Su, H.M., Guo, C.L., Chen, Y.C., 2011b. Porphyry Cu–Au–Mo–epithermal Ag–Pb–Zn–distal hydrothermal Au deposits in the Dexing area, Jiangxi province, East China – a linked ore system. Ore Geol. Rev. 43, 203–216.

Mao, J.W., Cheng, Y.B., Chen, M.H., Pirajno, F., 2013. Major types and time-space distribution of Mesozoic ore deposits in South China and their geodynamic settings. Miner. Deposita 48 (3), 267–294.

Meffre, S., Large, R.R., Scott, R., Woodhead, J., Chang, Z., Gilbert, S.E., Danyushevsky, L.V., Maslennikov, V., Hergt, J.M., 2008. Age and pyrite Pb-isotopic composition of the giant Sukhoi Log sediment-hosted gold deposit, Russia. Geochim. Cosmochim. Acta 72, 2377–2391.

Ohmoto, H., Goldhaber, M.B., 1997. Sulfur and carbon isotopes. In: Barnes, H.L. (Ed.), Geochemistry of Hydrothermal Ore Deposits. third ed. John Wiley and Sons, New York, pp. 517–611.

Ou-Yang, X.C., 2015. Geological and Geochemical Characteristics and Its Genesis of the Dongxiang Copper Deposit, Jiangxi Province. China University of Geosciences, Beijing, pp. 46–50 (Paper for master's degree, in Chinese with English abstract).

Paton, C., Woodhead, J.D., Hellstrom, J.C., Hergt, J.M., Greig, A., Maas, R., 2010. Improved laser ablation U-Pb zircon geochronology through robust down-hole fractionation correction. Geochem. Geophys. Geosyst. 11, 1525–2027.

Sack, P.J., Berry, R.F., Meffre, S., Falloon, T.J., Gemmell, J.B., Friedman, R.M., 2011. In situ location and U-Pb dating of small zircon grains in igneous rocks using laser ablation-inductively coupled plasma-quadrupole mass spectrometry. Geochem. Geophys. Geosyst. 12, 1–23.

Seton, M., Müller, R.D., 2008. Reconstructing the junction between Panthalassa and Tethys since the Early Cretaceous. In: PESA Eastern Australasian Basins Symposium III, Sydney, 14–17 September, earthbyte.org, pp. 263–266.

Shu, L.S., 2006. Predevonian tectonic is evolution of South China from Cathaysian block to Caledonian period folded orogenic belt. Geol. J. China Univ. 12, 418–431 (in Chinese with English abstract).

Shu, L.S., Zhou, X.M., 2002. Late Mesozoic tectonism of Southeast China. Geol. Rev. 48 (3), 249–260 (in Chinese with English abstract).

Smoliar, M.I., Walker, R.J., Morgan, J.W., 1996. Re–Os ages of group IIA, IIIA, IVA, and IVB iron meteorites. Science 271, 1099–1102.

Steiger, R.H., Jäger, E., 1977. Subcommission on geochronology: convention on the use of decay constants in geo- and cosmochronology. Earth Planet. Sci. Lett. 36, 359–362.

Sun, M.D., Xu, Y.G., Wilde, S.A., Chen, H.L., Yang, S.F., 2015. The Permian Dongfanghong island-arc gabbro of the Wandashan Orogen, NE China: implications for Paleo-Pacific subduction. Tectonophysics 659, 122–136.

Tang, Y.W., Xie, Y.L., Li, Y.X., Qiu, L.M., Liu, B.S., Li, Y., Zhang, X.X., Jiang, Y.C., Han, Y. D., 2012. Petrogeochemical and petrographic characteristics and genesis of Wushanguan complex body in Anji ore district, Zhejiang Province. Miner. Depos. 31 (4), 903–916 (in Chinese with English abstract).

Tang, Y.W., Xie, Y.L., Li, Y.X., Qiu, L.M., Zhang, X.X., Han, Y.D., Jiang, Y.C., 2013. LA–ICP–MS U-Pb ages, geochemical characteristics of the zircons from Wushanguan complex body in Anji mining area, northwestern Zhejiang and their geological significances. Geol. Rev. 59, 702–715 (in Chinese with English abstract).

Tang, Y.W., Li, X.F., Zhang, X.Q., Yang, J.L., Xie, Y.L., Lan, T.G., Huang, Y.F., Huang, C., Yin, R.C., 2015a. Some new data on the genesis of the Linghou Cu–Pb–Zn polymetallic deposit—based on the study of fluid inclusions and C–H–O–S–Pb isotopes. Ore Geol. Rev. 71, 248–262.

Tang, Y.W., Li, X.F., Xie, Y.L., Huang, C., Wei, H., Cai, J.L., Yin, Y.F., Qin, C.J., Liu, R., 2015b. Geology, geochemistry, and genesis of the Tongcun reduced porphyry Mo (Cu) deposit, NW Zhejiang Province, China. Acta Geol. Sin. (Engl. Ed.) 89 (3), 766–782.

Tian, J.H., Ni, P., Fan, J.G., 2001. Ore-forming fluid characteristics research of Yongping copper deposit. Contrib. Geol. Miner. Resour. Res. 16, 24–27 (in Chinese with English abstract).

Wang, Z.J., 1990. The exploration model for Jiande copper deposit. Miner. Resour. Geol. East China, 11–22 (In Chinese).

Wang, L., 2010. Metallogenic Model and Prospecting Potential in Dabaoshan Molybdenum Polymetallic Ore Deposit, North Guangdong Province. China University of Geosciences, Wuhan, pp. 53–86 (Paper for doctoral degree, in Chinese with English abstract).

Wang, Q., Zhao, Z.H., Jian, P., Xu, J.F., Bao, Z.W., Ma, J.L., 2004. SHRIMP zircon geochronology and Nd-Sr isotopic geochemistry of the Dexing granodiorite porphyries. Acta Petrol. Sin. 20 (2), 315–324 (in Chinese with English abstract).

Wang, Q., Xu, J.F., Jian, P., Bao, Z.W., Zhao, Z.H., Li, C.F., Xiong, X.L., Ma, J.L., 2006. Petrogenesis of adakitic porphyries in an extensional tectonic setting, Dexing, south China: implications for the genesis of porphyry copper mineralization. J. Petrol. 47 (1), 119–144.

Wang, G.G., Ni, P., Zhao, K.D., Liu, J.R., Xie, G.A., Xu, J.H., Zhang, Z.H., 2011. Comparison of fluid inclusions in coexisting sphalerite and quartz from Yinshan deposit, Dexing, Northeast Jiangxi Province. Acta Petrol. Sin. 27, 1387–1397 (in Chinese with English abstract).

Wang, L., Hu, M.A., Qu, W.J., Chen, K.X., Long, W.G., Yang, Z., 2012a. Zircon LA–ICP–MS U-Pb and molybdenite Re–Os dating of the Dabaoshan polymetallic deposit in northern Guangdong Province and its geological implications. Geol. China 39 (1), 29–42 (in Chinese with English abstract).

Wang, C.Y., Li, X.F., Xiao, R., Bai, Y.P., Yang, F., Mao, W., Jiang, S.K., 2012b. Elements mobilization of mineralized porphyry rocks during hydrothermal alteration at Zhushahong porphyry copper deposit, Dexing district, South China. Acta Petrol. Sin. 28, 3869–3886 (in Chinese with English abstract).

Wang, G.G., Ni, P., Wang, R.C., Zhao, K.D., Chen, H., Ding, J.Y., Zhao, C., Cai, Y.T., 2013a. Geological, fluid inclusion and isotopic studies of the Yinshan Cu–Au–Pb–Zn–Ag deposit, South China: implications for ore genesis and exploration. J. Asian Earth Sci. 74, 343–360.

Wang, H.Z., Zhang, D., Di, Y.J., Luo, P., Lv, L.Y., Dong, Y., Lu, J.H., 2013b. Hydrothermal potash feldspar Ar–Ar dating for Tieshajie copper deposit, Jiangxi Province. Acta Miner. Sin. S2, 613–614 (in Chinese).

Wang, G.G., Ni, P., Yao, J., Wang, X.L., Zhao, K.D., Zhu, R.Z., Xu, Y.F., Pan, J.Y., Li, L., Zhang, Y.H., 2015a. The link between subduction-modified lithosphere and the giant Dexing porphyry copper deposit, South China: constraints from high-Mg adakitic rocks. Ore Geol. Rev. 67, 109–126.

Wang, M., Bai, X.J., Hu, R.G., Cheng, S.B., Pu, Z.P., Qiu, H.N., 2015b. Direct dating of Cassiterite in Xitian tungsten-tin polymetallic deposit, South-East Hunan, by $^{40}Ar/^{39}Ar$ progressive crushing. Geotect. Metall. 39 (6), 1049–1060 (in Chinese with English abstract).

Wiedenbeck, M., Alle, P., Corfu, F., Griffin, W.L., Meier, M., Oberli, F., Vonquadt, A., Roddick, J.C., Speigel, W., 1995. 3 Natural zircon standards for U-Th–Pb, Lu–Hf, trace-element and REE analyses. Geostand. Newslett. 19, 1–23.

Wu, F.Y., Ge, W.C., Sun, D.Y., Guo, C.L., 2003. Discussions on the lithospheric thinning in eastern China. Earth Sci. Front. 10 (3), 51–60 (in Chinese with English abstract).

Xiao, Q.H., Li, Y., Feng, Y.F., Qiu, R.Z., Zhang, Y., 2010. A preliminary study of the relationship between Mesozoic lithosphere evolution in eastern China and the subduction of the Pacific plate. Geol. China 37 (4), 1092–1101 (in Chinese with English abstract).

Xie, Y.L., Tang, Y.W., Li, Y.X., Qiu, L.M., Liu, B.S., Li, Y., Zhang, X.X., Han, Y.D., Jiang, Y. C., 2012a. Petrochemistry, chronology and ore-forming geological significance of fine crystalline granite in Anji polymetallic deposit of Zhejiang Province. Miner. Depos. 31 (4), 891–902 (in Chinese with English abstract).

Xie, Y.L., Tang, Y.W., Dominy, S.C., Li, Y.X., Zhang, X.X., 2012b. Re–Os isotope dating of molybdenite and significance of Anji Pb–Zn polymetallic deposit in Zhejiang Province of China. In: Proceedings of the 34th International Geological Congress, Brisbane, Australia, p. 3370.

Xu, Y.T., 1998. Early metallogenic the Yongping Cu–W geochemistry in massive sulfide deposit, Jiangxi. Geotect. Metall. 22, 55–64 (in Chinese with English abstract).

Xu, Z.Z., Zhang, H.T., Jiang, Y., 1981. Study on the conditions of structure to control the ore in Jiande copper deposit. J. Chengdu Inst. Geol. 2, 6–17 (in Chinese with English abstract).

Xu, K.Q., Wang, H.N., Zhou, J.P., Zhu, J.C., 1996. A discussion on the exhalative sedimentary massive sulfide deposits of South China. Geol. J. China Univ. 2 (3), 241–256 (in Chinese with English abstract).

Xu, D.M., Lin, Z.Y., Long, W.G., Zhang, K., Wang, L., Zhou, D., Huang, H., 2012. Research history and current situation of Qinzhou-Hangzhou metallogenic belt, South China. Geol. Miner. Resour. South China 28 (4), 277–289 (in Chinese with English abstract).

Xu, D.M., Lin, Z.Y., Luo, X.Q., Zhang, K., Zhang, X.H., Huang, H., 2015. Metallogenetic series of major metallic deposits in the Qinzhou-Hangzhou metallogenic belt. Earth Sci. Front. 22 (2), 007–124 (in Chinese with English abstract).

Yamasaki, S., Sawada, R., Ozawa, A., Tagami, T., Watanabe, Y., Takahashi, E., 2011. Unspiked K-Ar dating of Koolau lavas, Hawaii: evaluation of the influence of weathering/alteration on age determinations. Chem. Geol. 287, 41–53.

Yang, M.G., Mei, Y.W., 1997. Characteristics of geology and metallization in the Qinzhou-Hangzhou paleoplate juncture. Geol. Miner. Resour. South China, 52–59 (in Chinese with English abstract).

Yang, B., Luo, L.Y., Luo, S.J., 2000. Discussion on the genesis of Fozichong lead-zinc ore field. Guangxi Geol. 13 (1), 21–27 (in Chinese with English abstract).

Yang, M.G., Huang, S.B., Lou, F.S., Tang, W.X., Mao, S.B., 2009. Lithospheric structure and large-scale metallogenic process in Southeast China continental area. Geol. China 36, 528–543 (in Chinese with English summary).

Yu, Y.P., 2010. Geological characteristics of deposit and distribution law of main ore elements in Songkengwu ore block of Zhejiang Jiande copper mine. Miner. Resour. Geol. 24 (5), 407–413 (in Chinese with English abstract).

Zhang, J.F., Zhang, G.Y., 2009. A summary of the application of lead isotope to study on ore deposits and ore exploration. Contrib. Geol. Miner. Resour. Res. 24, 322–328 (in Chinese with English abstract).

Zhang, J.J., Mei, Y.P., Wang, D.H., Li, H.Q., 2008. Isochronology study on the Xianglushan scheelite deposit in north Jiangxi province and its geological significance. Acta Geol. Sin. 82 (7), 927–931 (in Chinese with English abstract).

Zhang, B.T., Wu, J.Q., Ling, H.F., Chen, P.R., 2010. Petrological discrimination between primary and secondary muscovites and its geological implications: a case study of Fucheng peraluminous granite pluton in southern Jiangxi. Acta Petrol. Mineral. 29 (3), 225–234 (in Chinese with English abstract).

Zhang, S.M., Xiao, Y.F., Wang, Q., Zhang, X.H., Yang, L., Wang, Y.B., Zhang, C.M., 2013. Re–Os dating of molybdenite from the Tongcun porphyry molybdenum deposit in western Zhejiang Province and its geological implications. Geol. Explor. 49 (1), 0050–0057 (in Chinese with English abstract).

Zhang, J.F., Chen, M.J., Xie, H.S., Gong, R.J., Zhu, B.X., Wang, L.W., Xu, X.M., 2015. Metallogenic types, age and prospecting potential of iron polymetallic deposits associated with igneous rocks at Lizhu District, Northwestern Zhejiang Province. Geotect. Metall. 39 (4), 647–657 (in Chinese with English abstract).

Zhao, H.J., Yu, Z.F., Guan, B.T., Hu, Y.G., Xu, M.J., 2012. Geochronology and petrogenesis of biotite granite from the Gaocheng Pb–Zn–Ag deposit, in western Guangdong Province, China. Acta Petrol. Sin. 28 (12), 3951–3966 (in Chinese with English abstract).

Zhao, H.J., Yu, Z.F., Han, X.Q., Zheng, W., 2016. Magmatic hydrothermal superimposition in Dajiangping S (Pb–Zn) deposit, Guangdong Province: Rb–Sr isochron age and sulfur isotope evidence. Miner. Depos. 35 (4), 795–808 (in Chinese with English abstract).

Zheng, Y.F., Zhao, Z.F., Chen, Y.X., 2013. Continental subduction channel processes: plate interface interaction during continental collision. Chin. Sci. Bull. 58, 4371–4377.

Zhong, L., Liu, L., Xia, B., Li, J., Lin, X., Xu, L., Lin, L., 2010. Re–Os geochronology of molybdenite from Yuanzhuding porphyry Cu–Mo deposit in South China. Resour. Geol. 60 (4), 389–396.

Zhong, L., Li, J., Peng, T., Xia, B., Liu, L., 2013. Zircon U-Pb geochronology and Sr–Nd–Hf isotopic compositions of the Yuanzhuding granitoid porphyry within the Shi-Hang Zone, South China: petrogenesis and implications for Cu–Mo mineralization. Lithos 177, 402–415.

Zhou, J.Y., Yu, Z.C., 1983. Characteristics of the Jiande copper deposit in Zhejiang province and ore forming fluid migration. J. Chengdu Inst. Geol. 4, 1–22 (in Chinese with English abstract).

Zhou, X.M., Sun, T., Shen, W.Z., Shu, L.S., Niu, Y.L., 2006. Petrogenesis of Mesozoic granitoids and volcanic rocks in South China: a response to tectonic evolution. Episodes 29, 26–33.

Zhou, Y.Z., Zeng, C.Y., Li, H.Z., An, Y.F., Liang, J., Lü, W.C., Yang, Z.J., He, J.G., Shen, W.J., 2012. Geological evolution and ore prospecting targets in southern segment of Qinzhou Bay-Hangzhou Bay juncture orogenic belt, southern China. Geol. Bull. China 31 (2/3), 486–491 (in Chinese with English abstract).

Zhou, Q., Jiang, Y.H., Zhang, H.H., Liao, S.Y., Jin, G.D., Zhao, P., Jia, R.Y., Liu, Z., 2013. Mantle origin of the Dexing porphyry copper deposit, SE China. Int. Geol. Rev. 55, 337–349.

Zhou, Y., Liang, X., Wu, S., Cai, Y., Liang, X., Shao, T., Wang, C., Fu, J.G., Jiang, Y., 2015. Isotopic geochemistry, zircon U-Pb ages and Hf isotopes of A-type granites from the Xitian W-Sn deposit, SE China: constraints on petrogenesis and tectonic significance. J. Asian Earth Sci. 105, 122–139.

Zhou, Y.Z., Zheng, Y., Zeng, C.Y., Liang, J., 2015. On the understanding of Qinzhou Bay-Hangzhou Bay metallogenic belt, South China. Earth Sci. Front. 22 (2), 001–006 (in Chinese with English abstract).

Zhu, Y.D., Ye, X.F., Zhang, D.H., Wang, K.Q., Wang, C.Y., Yin, X.B., 2014. Petrochemistry, SHRIMP dating and Sr–Nd isotopic constraints on the origin of the Kaihua porphyry Mo (Cu) deposit, Zhejiang Province. Earth Sci. Front. 21, 01–014 (in Chinese with English abstract).

Zuo, C.H., Miao, B.H., Zhao, Z.X., Xu, Z.W., Lu, J.J., Lu, R., Chen, J.Q., 2014. A study on the isotopic geochemistry of Kangjiawan lead-zinc deposit, Changning county, Hunan Province, China. Acta Mieral. Sin. 34, 351–359 (in Chinese with English abstract).